Dept. of Biomedical Engineering and Computational Science

Multimodal applications of functional near-infrared spectroscopy

Tiina Näsi

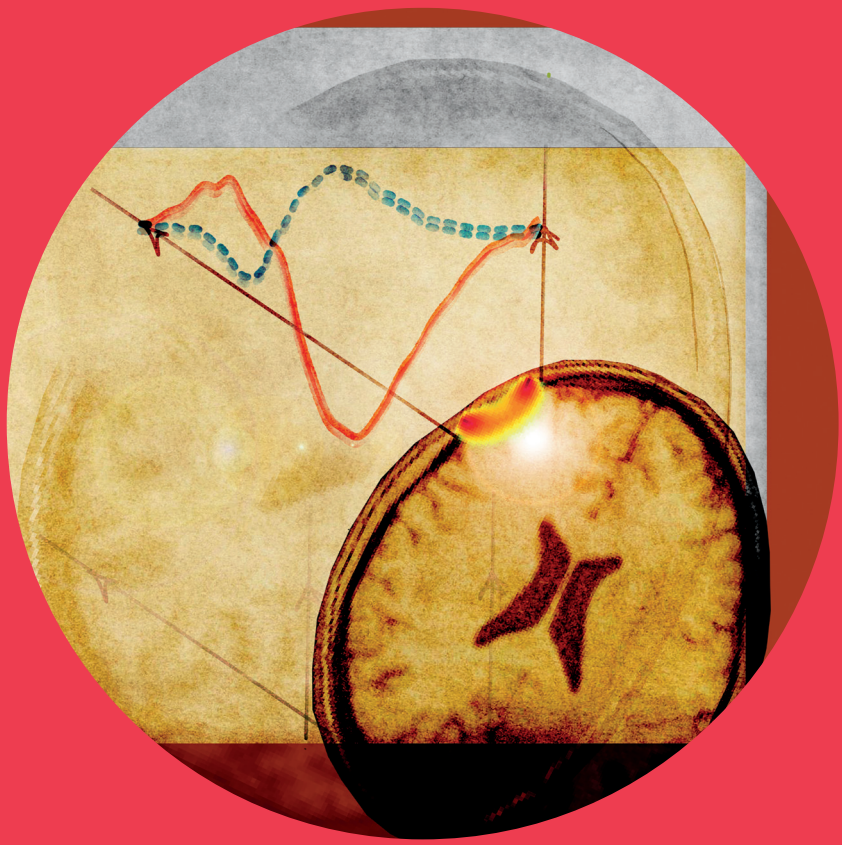

Aalto University

DOCTORAL DISSERTATIONS

Aalto University publication series
DOCTORAL DISSERTATIONS 45/2013

Multimodal applications of functional near-infrared spectroscopy

Tiina Näsi

A doctoral dissertation completed for the degree of Doctor of Science (Technology) to be defended, with the permission of the Aalto University School of Science, at a public examination held at the Auditorium F239a of the school on 12 April 2013 at 12.

Aalto University
School of Science
Dept. of Biomedical Engineering and Computational Science

Supervising professor
Academy Prof. Risto Ilmoniemi

Thesis advisor
Academy Prof. Risto Ilmoniemi

Preliminary examiners
Docent Tanja Tarvainen, University of Eastern Finland, Finland
Prof. Sergio Fantini, Tufts University, USA

Opponent
Prof. Arno Villringer, Max Planck Institute for Human Cognitive and Brain Sciences, Germany

Aalto University publication series
DOCTORAL DISSERTATIONS 45/2013

ISBN 978-952-60-5069-0 (printed)
ISBN 978-952-60-5070-6 (pdf)
ISSN-L 1799-4934
ISSN 1799-4934 (printed)
ISSN 1799-4942 (pdf)
http://urn.fi/URN:ISBN:978-952-60-5070-6

Unigrafia Oy
Helsinki 2013

Finland

441 697
Printed matter

Aalto University

Abstract

Aalto University, P.O. Box 11000, FI-00076 Aalto www.aalto.fi

Author
Tiina Näsi

Name of the doctoral dissertation
Multimodal applications of functional near-infrared spectroscopy

Publisher School of Science

Unit Department of Biomedical Engineering and Computational Science

Series Aalto University publication series DOCTORAL DISSERTATIONS 45/2013

Field of research Biomedical engineering and biophysics

Manuscript submitted 11 December 2012 **Date of the defence** 12 April 2013

Permission to publish granted (date) 24 January 2013 **Language** English

☐ **Monograph** ☒ **Article dissertation (summary + original articles)**

Abstract

With the population of the world getting older, the number of patients suffering from brain disorders is increasing. To tackle this challenge, safe, affordable, and easy-to-use methods for screening, diagnosing, and treating these disorders are needed. Functional near-infrared spectroscopy (fNIRS), an optical method for monitoring blood circulatory changes related to brain activity, fulfills these requirements. However, it is still not in wide clinical use—partly because the measured physiological phenomena are complex and therefore sometimes difficult to interpret.

This Thesis demonstrates that fNIRS can be combined with other modalities to investigate phenomena that cannot be studied with separate recordings. Such multimodal measurements aid in characterizing and understanding physiological artifacts in fNIRS signals, and they can be used in various clinical applications. This Thesis focuses on the applications of monitoring sleep and characterizing effects of transcranial magnetic stimulation (TMS), a technique for diagnosing and treating various neurological and psychiatric disorders.

The results in sleep monitoring show that circulatory changes recorded with fNIRS complement previous knowledge of the electrophysiological characteristics of sleep. Furthermore, some observations may be related to harmful effects of sleep disorders on the vasculature. In awake subjects, the developed multimodal method can serve in investigating neurovascular coupling. Altogether, the work contributes to methodology and analysis techniques for monitoring circulation during sleep and establishes a solid base for applying them in clinical settings.

The results in recording effects of TMS suggest that TMS-evoked fNIRS responses should be interpreted with caution; fNIRS signals contain physiological artifacts during TMS. Furthermore, fNIRS signals are affected by changes in scalp circulation during mental and physical stress, but this problem can be alleviated by separating the changes in scalp and brain circulation with diffuse optical tomography. The reported observations increase the understanding about the origin of fNIRS signals, contribute to techniques for removing artifacts, and thus advance the usability of fNIRS in monitoring effects of TMS or sleep.

Keywords near-infrared spectroscopy, diffuse optical tomography, transcranial magnetic stimulation, sleep, hemodynamic monitoring, physiological artifact

ISBN (printed) 978-952-60-5069-0 **ISBN (pdf)** 978-952-60-5070-6

ISSN-L 1799-4934 **ISSN (printed)** 1799-4934 **ISSN (pdf)** 1799-4942

Location of publisher Espoo **Location of printing** Helsinki **Year** 2013

Pages 129 **urn** http://urn.fi/URN:ISBN:978-952-60-5070-6

A? Aalto-yliopisto

Tiivistelmä

Aalto-yliopisto, PL 11000, 00076 Aalto www.aalto.fi

Tekijä
Tiina Näsi

Väitöskirjan nimi
Toiminnallinen lähi-infrapunaspektroskopia monimenetelmäsovelluksissa

Julkaisija Perustieteiden korkeakoulu

Yksikkö Lääketieteellisen tekniikan ja laskennallisen tieteen laitos

Sarja Aalto University publication series DOCTORAL DISSERTATIONS 45/2013

Tutkimusala Lääketieteellinen tekniikka ja biofysiikka

Käsikirjoituksen pvm 11.12.2012 **Väitöspäivä** 12.04.2013

Julkaisuluvan myöntämispäivä 24.01.2013 **Kieli** Englanti

☐ **Monografia** ☒ **Yhdistelmäväitöskirja (yhteenveto-osa + erillisartikkelit)**

Tiivistelmä

Aivosairauksista kärsivien ihmisten määrä kasvaa maailman väestön ikääntyessä. Samalla myös näiden sairauksien seulontaan, diagnosointiin ja hoitoon käytettävien turvallisten, edullisten ja helppokäyttöisten menetelmien tarve lisääntyy. Toiminnallinen lähi-infrapunaspektroskopia (fNIRS) täyttää nämä vaatimukset. Se on menetelmä, jolla mitataan optisesti aivotoiminnan seurauksena aivojen verenkierrossa tapahtuvia muutoksia. Hyvistä ominaisuuksistaan huolimatta fNIRS ei ole kuitenkaan laajassa kliinisessä käytössä. Tämä johtuu osittain siitä, että menetelmän mittaamat fysiologiset ilmiöt ovat monimutkaisia ja siten toisinaan hankalia tulkita.

Tämä väitöskirja osoittaa, että yhdistämällä fNIRS muihin menetelmiin voidaan tutkia ilmiöitä, joihin yksittäisillä menetelmillä ei päästä käsiksi. Tällaiset mittaukset auttavat luonnehtimaan ja ymmärtämään fNIRS-signaaleita. Lisäksi niillä on monia kliinisiä sovelluskohteita, joista tämä väitöskirja keskittyy unen seurantaan ja aivojen magneettistimulaation (TMS) vaikutusten mittaamiseen. TMS:ää voidaan käyttää monien neurologisten ja psykiatristen sairauksien diagnosointiin ja hoitoon.

Unen seurantaan liittyvät tulokset osoittavat, että fNIRS:llä mitatut verenkierron muutokset täydentävät aiempaa elektrofysiologisten mittausten perusteella saatua tietämystä aivotoiminnan piirteistä unen aikana. Lisäksi osa havainnoista saattaa olla yhteydessä unisairauksien aiheuttamiin haitallisiin muutoksiin verisuonistossa. Hereillä olevilla koehenkilöillä samoja tekniikoita voidaan soveltaa hermoston ja verisuonten välisen kytkennän tutkimiseen. Kaiken kaikkiaan työssä kehitetyt menetelmät verenkierron monitorointiin unen aikana luovat vankan pohjan niiden käytölle kliinisessä ympäristössä.

Tulokset TMS:n vaikutusten mittaamisesta viittaavat siihen, että TMS:n aikaisten fNIRS-signaalien tulkinnassa tulee noudattaa erityistä varovaisuutta; fNIRS-signaalit sisältävät fysiologisia häiriötä TMS:n aikana. Lisäksi muutokset päänahan verenkierrossa häiritsevät aivoperäisten fNIRS-signaalien mittaamista fyysisen ja henkisen kuormituksen aikana, mutta häiriöitä voidaan lieventää erottelemalla pinnasta ja aivoista lähtöisin olevat signaalit diffuusin optisen tomografian avulla. Väitöskirjassa esitetyt havainnot täydentävät aiempaa tietämystä fNIRS-signaalien alkuperästä, auttavat häiriöiden poistossa ja näin ollen edistävät fNIRS:n käytettävyyttä TMS:n vaikutusten ja unen mittaamisessa.

Avainsanat lähi-infrapunaspektroskopia, diffuusi optinen kuvantaminen, aivojen magneettistimulaatio, uni, verenkierron seuranta, fysiologinen häiriö

ISBN (painettu) 978-952-60-5069-0 **ISBN (pdf)** 978-952-60-5070-6

ISSN-L 1799-4934 **ISSN (painettu)** 1799-4934 **ISSN (pdf)** 1799-4942

Julkaisupaikka Espoo **Painopaikka** Helsinki **Vuosi** 2013

Sivumäärä 129 **urn** http://urn.fi/URN:ISBN:978-952-60-5070-6

Preface

This Thesis is a result of research carried out at the Department of Biomedical Engineering and Computational Science (BECS) of Aalto University, formerly the Laboratory of Biomedical Engineering of Helsinki University of Technology (HUT). The experiments have been conducted in the BioMag Laboratory, Helsinki University Central Hospital. Grants from the Finnish Cultural Foundation, the Instrumentarium Science Foundation, the International Graduate School in Biomedical Engineering and Medical Physics, and Helsinki University of Technology have made the work financially possible. Throughout this doctoral project, I have collaborated with a number of scientists and medical doctors. I am indebted to each one of them for learning so much during these years, being able to work in interesting projects, and getting help whenever needed.

I wish to express my gratitude to my supervisor Prof. Risto Ilmoniemi, who has given me the opportunity to work at BECS and more importantly taught me scientific thinking. I would like to thank him for his willingness to share knowledge and for being such an encouraging supervisor. I am also grateful to my former supervisor Prof. Pekka Meriläinen, who supported me in the early stages of my doctoral studies. Furthermore, I am thankful to Docent Jyrki Mäkelä for making it possible to use the state-of-the-art equipments at BioMag.

I am fortunate to have worked very closely with two competent scientists Dr. Hanna Mäki and Dr. Jaakko Virtanen. It has been a pleasure to share our academic lives and beyond with Hanna. I am grateful to Jaska for having introduced me to the interesting and fruitful project regarding sleep hemodynamics.

I also wish to convey my gratitude to all the other past and present members of the optical imaging group—Dr. Ilkka Nissilä, Dr. Petri Hiltunen, Kalle Kotilahti, Dr. Tommi Noponen, Dr. Juha Heiskala, Lauri Lipiäinen,

and many others. The help and support from the group members at various phases of my doctoral project have been of great importance. It has also been a pleasure to collaborate with medical doctors Dr. Jussi Toppila, Docent Tapani Salmi, and Dr. Petri Haapalahti, who have provided their medical expertise whenever needed.

I am fortunate to have spent many years at BECS in such an inspiring and pleasant environment—for this I want to thank all my colleagues and friends at BECS. Also, the kind staff and researchers at BioMag deserve many compliments for helping with whatever practical problems we have encountered while conducting experiments. Moreover, I acknowledge our persistent and open-minded subjects—without their help and time the research would not have been possible.

I greatly appreciate the preliminary examiners Docent Tanja Tarvainen and Prof. Sergio Fantini for their suggestions to improve this manuscript. I also thank Dr. Ilkka Nissilä, Dr. Jaakko Virtanen, Dr. Jaakko Nieminen, Dr. Petri Hiltunen, and Dr. Hanna Mäki for their comments. Furthermore, I devote thanks to Daniel Arévalo, who has made the artwork in the cover of this book.

People outside of my academic life have also played an important part in the completion of this Thesis. I want to thank all my friends—let them be old schoolmates, fellow students from HUT, friends from hobbies, Mexicans, friends through other reasons, or my sister Anni—for taking my mind off work to enjoy life outside academia as well. The unconditional support from my parents during my 20-years-long journey of education has been invaluable. Finally, I am forever grateful to Gerardo for acting like a Mexican, following any weird plans that friends suggest, and ending up as a subject in one of our experiments. I wish to thank you for all the invaluable support and great time that have followed.

Espoo, February 22, 2013,

Tiina Näsi

Contents

List of publications

This Thesis consists of an overview and of the following publications, which are referred to in the text by their Roman numerals.

I T. Näsi, K. Kotilahti, T. Noponen, I. Nissilä, L. Lipiäinen, and P. Meriläinen. Correlation of visual-evoked hemodynamic responses and potentials in human brain. *Experimental Brain Research*, 202:561–570, May 2010.

II T. Näsi, J. Virtanen, T. Noponen, J. Toppila, T. Salmi, and R. J. Ilmoniemi. Spontaneous hemodynamic oscillations during human sleep and sleep stage transitions characterized with near-infrared spectroscopy. *PLoS ONE*, 6:e25415, Oct 2011.

III T. Näsi, J. Virtanen, J. Toppila, T. Salmi, and R. J. Ilmoniemi. Cyclic alternating pattern is associated with cerebral hemodynamic variation: a near-infrared spectroscopy study of sleep in healthy humans. *PLoS ONE*, 7:e46899, Oct 2012.

IV T. Näsi, H. Mäki, K. Kotilahti, I. Nissilä, P. Haapalahti, and R. J. Ilmoniemi. Magnetic-stimulation-related physiological artifacts in hemodynamic near-infrared spectroscopy signals. *PLoS ONE*, 6:e24002, Aug 2011.

V T. Näsi, H. Mäki, P. Hiltunen, J. Heiskala, I. Nissilä, K. Kotilahti, and R. J. Ilmoniemi. Effect of task-related extracerebral circulation on diffuse optical tomography: experimental data and simulations on the forehead. *Biomedical Optics Express*, 4:412–426, Mar 2013.

Author's contribution

Publication I: "Correlation of visual-evoked hemodynamic responses and potentials in human brain"

The author had the main responsibility for planning and executing the experiments, analyzing the data, and interpreting the results. She is the principal writer of the article.

Publication II: "Spontaneous hemodynamic oscillations during human sleep and sleep stage transitions characterized with near-infrared spectroscopy"

The author analyzed the optical and cardiovascular data together with the second author with whom she also shared the main responsibility for interpreting the results. She assisted the second author in writing the first version of the article and in editing the article based on the input from the other authors. She shares the first authorship with the second author.

Publication III: "Cyclic alternating pattern is associated with cerebral hemodynamic variation: a near-infrared spectroscopy study of sleep in healthy humans"

The author had the main responsibility for analyzing the optical and cardiovascular data as well as for interpreting the results. She is the principal writer of the article. She shares the first authorship with the second author.

Publication IV: "Magnetic-stimulation-related physiological artifacts in hemodynamic near-infrared spectroscopy signals"

The author, together with the second author, had the main responsibility for planning and executing the experiments, analyzing the data, interpreting the results, and writing the article. She shares the first authorship with the second author.

Publication V: "Effect of task-related extracerebral circulation on diffuse optical tomography: experimental data and simulations on the forehead"

The author shared the main responsibility for planning and executing the experiments and analyzing the data. She had the main responsibility for making the simulations and interpreting the results. She is the principal writer of the article.

List of abbreviations

$\Delta[X]$	change in $[X]$
$[X]$	concentration of chromophore X
BOLD	blood-oxygen-level-dependent signal
CAP	cyclic alternating pattern
CBF	cerebral blood flow
DOT	diffuse optical tomography
DPF	differential path-length factor
ECG	electrocardiography
EEG	electroencephalography
EMG	electromyography
EOG	electrooculography
fMRI	functional MRI
fNIRS	functional NIRS
HbO_2	oxyhemoglobin
HbR	deoxyhemoglobin
HbT	total hemoglobin
MRI	magnetic resonance imaging
NIR	near infrared
NIRS	near-infrared spectroscopy
PCA	principal component analysis
PET	positron emission tomography
PPG	photoplethysmogram
PPGamp	amplitude of the PPG waveform
PSG	polysomnography
PTT	pulse transit time
REM	rapid-eye-movement sleep
SNR	signal-to-noise ratio
SpO_2	arterial oxygen saturation
TMS	transcranial magnetic stimulation

1. Introduction

1.1 Background

The proportion of people suffering from brain dysfunction or diseases is increasing, as people tend to live longer than in the past. At the moment, roughly one fifth of the population of Finland is affected by a disorder of the brain [171], and the related costs for the society are great. Mood disorders alone have been estimated to cost over one billion euros in Finland in 2010, and sleep disorders cast on top of that another 300 million euro bill [76]. To tackle the challenge of an increasing number of brain disorders, safe, affordable, and easy-to-use methods for diagnosing, treating, and screening are needed [204]. New technology and methods may not only help medical doctors diagnose brain disorders and monitor treatment, they may also improve patients' quality of life through earlier diagnosis and a potential shift from treating disease towards prevention. Furthermore, new methods for measuring brain activity can increase our knowledge on brain function in order to develop better ways to treat these disorders.

One relatively new method for measuring brain function which fulfills the technical requirements of being portable, relatively cheap, and safe is functional near-infrared spectroscopy (fNIRS) [101]. It records changes in blood oxygenation and volume (hemodynamics) related to brain activity by measuring attenuation of light in the head. It is noninvasive, quiet, and so safe that it can even be applied to study the developing brain of infants [35, 120]. In addition, it can be used in a natural environment, tolerates small movements, and is suitable for monitoring purposes. One of its great advantages is its suitability for multimodal measurements. These aforementioned properties make fNIRS a compelling alternative

to other brain imaging modalities. However, fNIRS is still not widely applied in the clinic or research because methodological and technological limitations in combination with complexity of the underlying physiology make the signals often difficult to interpret [56, 90, 142, 203].

The objective of the work in this Thesis was to combine fNIRS with other modalities to investigate phenomena that cannot be studied with separate modalities, and to facilitate the interpretation of fNIRS signals. The goal was to develop combined methods that would be beneficial in diagnosing patients and monitoring their treatment. More specifically, the focus was in methods that could be eventually applied for monitoring sleep and effects of transcranial magnetic stimulation (TMS), a technique for diagnosing and treating various neurological and psychiatric disorders, e.g., depression [200, 201].

1.2 Aims

This Thesis consists of Publications I–V with the following aims:

1. To combine electroencephalography (EEG) and other recordings of polysomnography (PSG) with fNIRS.

   Publication I: To demonstrate the feasibility of simultaneous EEG and fNIRS in awake subjects for studying neurovascular coupling.

   Publications II and III: To characterize cerebral and systemic hemodynamics during natural sleep with simultaneous PSG/fNIRS.

2. To understand physiological artifacts in fNIRS to facilitate the development of methods for evaluating effects of TMS with fNIRS.

   Publication IV: To demonstrate that TMS-induced brain activity does not fully explain TMS-evoked changes in fNIRS signals and to discuss the origin of the physiological artifacts.

   Publication V: To characterize the effect of scalp circulation on diffuse optical tomography (DOT) reconstructions from fNIRS signals during physically and mentally demanding tasks.

2. Optical measurement of cerebral hemodynamics

2.1 Chapter overview

This chapter introduces the basics of fNIRS and DOT. It also presents fNIRS instrumentation in general and explains issues related to data interpretation. Lastly, it describes the fNIRS instrumentation and analysis methods used in this work.

2.2 Functional near-infrared spectroscopy (fNIRS)

Near-infrared spectroscopy (NIRS) is a method that records concentrations of chromophores, i.e., light-absorbing substances, with near-infrared (NIR) light. When NIRS is applied for studying hemodynamics related to brain activity, it is often called fNIRS. The fNIRS measurement is based on five physiological and physical principles: (1) cerebral blood flow (CBF) increases in active brain areas, (2) hemoglobin molecules of red blood cells absorb NIR light, (3) optical properties of hemoglobin depend on its oxygenation level, (4) tissue is relatively transparent to NIR light, and (5) NIR light is scattered strongly in all directions in tissue. These five principles are discussed in more detail in the following paragraphs.

Reacting to the increased energy consumption of an active brain area, CBF increases locally to supply nutrients and oxygen to the tissue (Principle 1) [155, 158]. The CBF rises more than the oxygen demand, resulting in an elevated blood oxygenation level in the active area [65]. Furthermore, the blood volume increases [33, 122]. These hemodynamic changes coupled to the neuronal activity are the basis of some functional neuroimaging methods, such as fNIRS and functional magnetic resonance imaging (fMRI) [155].

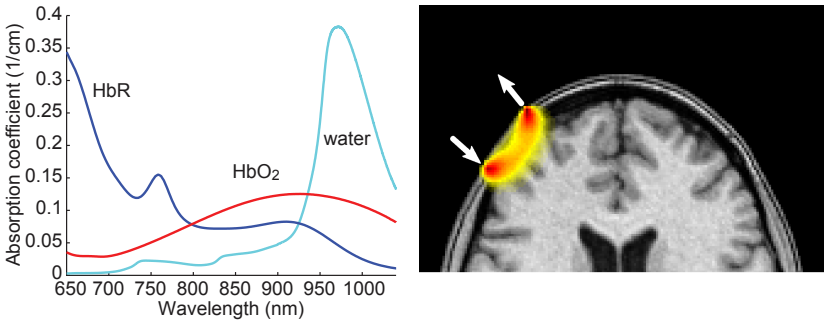

Figure 2.1. (a) Absorption coefficients of the major chromophores of tissue. The proportion of water in the tissue is assumed to be 75% and the hemoglobin concentrations 40 μM. (Data from Refs. [38] and [86]) (b) The banana-shaped sensitivity volume of fNIRS measurement. The source and detector fibers are depicted with white arrows (separation: 3.6 cm). The darker the yellow/red color, the higher the probability that the detected light has traversed the area. (Simulated data from Publication V)

Hemoglobin, the oxygen-carrying molecule of the blood, absorbs NIR light (Principle 2). Thus, the more blood the probed volume contains, the less light passes through it. Furthermore, the absorption of light depends on the oxygenation level of the blood (Principle 3, Fig. 2.1a); deoxyhemoglobin (HbR) absorbs more red light than oxyhemoglobin (HbO_2) [38], meaning that oxygen-deficient blood appears less red than oxygen-rich blood. To summarize Principles 1–3, neuronal activity generates changes in blood oxygenation and volume which in turn alter the absorption of light in the brain.

The NIR range of the spectrum (650–950 nm) is especially good for detecting blood-oxygen-level-dependent light absorption changes because it provides the so-called optical window of tissue (Principle 4). The optical window is limited by the high absorption coefficients of hemoglobin and melanin at shorter wavelengths and of water at longer wavelengths (Fig. 2.1a) [45]. In the optical window, the absorption is low which enables the light to penetrate deeper into tissue than outside the optical window. Therefore, NIR light transmitted to the tissue through an optical fiber placed on the scalp surface can reach the brain tissue, whereas light of other wavelengths gets mostly absorbed already in the surface layers.

The NIR light is scattered diffusively in all directions in the head (Principle 5), making it possible to measure light attenuation on the scalp surface a few centimeters apart from the source fiber. The sensitivity volume of the light is shaped like a banana (Fig. 2.1b); the longer the distance between the source fiber and the detection point, the deeper the banana-shape reaches in the tissue [44, 62, 139].

2.3 Modified Beer–Lambert law

The relation between the light attenuation in the illuminated tissue and the concentration of HbO_2 and HbR ([HbO_2] and [HbR]) can be modeled with the modified Beer–Lambert law when the concentrations of the chromophores are relatively small [38, 55]:

$$A(t) = \ln\left(\frac{I_0}{I(t)}\right) = A^* + G + \sum_{i=\mathrm{HbO_2,HbR}} \epsilon_i \cdot c_i(t) \cdot d \cdot B, \qquad (2.1)$$

where A is the attenuation, I_0 the light intensity entering the tissue, I the detected light intensity, A^* time-invariant attenuation caused by other chromophores besides HbO_2 and HbR, G a time-invariant term representing unknown scattering losses, ϵ_i and c_i the specific absorption coefficient and the concentration of chromophore i, respectively, d the geometrical distance between the illumination and detection point, and B the differential path-length factor (DPF). DPF represents the factor by which the distance traveled by light increases as a consequence of scattering, as compared to the geometrical distance between the illumination and detection point. Its value is usually between 5 and 6 in the adult head depending slightly on the wavelength [51, 195]. It can be measured with certain fNIRS instrumentation [6, 45]. The values for the specific absorption coefficients can be found in the literature [38].

The modified Beer–Lambert law serves for estimating changes in [HbO_2] and [HbR] (Δ[HbO_2] and Δ[HbR]), when the light attenuation is recorded with multiple wavelengths. Absolute concentrations of the chromophores cannot be obtained without additional information because of the unknown scattering losses in the tissue, represented by G in Eq. 2.1 [55]. Usually, Δ[HbO_2] and Δ[HbR] are reported for each fNIRS channel, i.e., a source–detector pair. Sometimes also the change in total hemoglobin concentration (Δ[HbT]), i.e., the sum of Δ[HbO_2] and Δ[HbR], is of interest because it is proportional to the blood volume change in the sampled tissue when the hematocrit is constant [19].

The modified Beer–Lambert law assumes the concentration of other chromophores besides HbO_2 and HbR as well as the scattering properties of the probed volume to be constant during the measurement. These assumptions are reasonable because the concentrations of the strongest absorbers, water and lipids, are unlikely to change as rapidly as [HbO_2] and [HbR] [55]. Furthermore, macroscopic and microscopic boundaries of

tissue structures that cause light scattering do not change considerably within the timescale of the measurement [55].

A more questionable assumption of the modified Beer–Lambert law is that the sampled medium is homogeneous. In reality, the head is a heterogeneous structure consisting of several compartments, which include the scalp, skull, cerebrospinal fluid, gray matter, and white matter, along with microscopic structures within all these compartments. The heterogenous structure of the head causes the light to traverse other tissue types besides brain tissue when it is guided into the head. Thus, the partial path length of the light in the brain is smaller than the total path length in the head, causing changes occurring in the brain circulation to produce smaller estimated $\Delta[HbO_2]$ and $\Delta[HbR]$ than what they are in reality [17, 18, 176]. This phenomenon is called the partial volume effect. Another related phenomenon is the differential sensitivity effect, which arises from the wavelength-dependency of the spatial sensitivity of the measurement and causes cross-talk between estimated $\Delta[HbO_2]$ and $\Delta[HbR]$ [17, 18, 176, 192]. The differential sensitivity effect can be minimized by selecting the measurement wavelengths appropriately [17, 176, 193, 207]. A third issue arises from the assumption that changes occur homogeneously in the probed volume: as the light traverses also the scalp, changes in the scalp circulation contribute to $\Delta[HbO_2]$ and $\Delta[HbR]$, which therefore do not solely represent changes in the cerebral hemodynamics. This issue is explained in more detail in Section 2.6.

2.4 Diffuse optical tomography (DOT)

Besides obtaining $\Delta[HbO_2]$ and $\Delta[HbR]$ in separate channels as in fNIRS, optical signals from multiple overlapping channels enable reconstructing images of optical properties of the tissue. This is called DOT [4, 16, 72].

In DOT, light propagation in the tissue is modeled with the radiative transfer equation or its diffusion approximation [4, 5, 16, 134]. Reconstructing optical properties of the probed tissue with these models is an ill-posed inverse problem: the reconstructions are highly sensitive to errors in the measurement data on the surface of the tissue and to a discrepancy between the data and the model. Moreover, the problem is non-unique, i.e., there are many possible distributions of optical properties that can give rise to the same measurement data [4, 7, 72].

In practice, the forward problem of DOT can be linearized:

$$\Delta y = J\Delta x, \tag{2.2}$$

where Δy is the change in measurement data, Δx the change in optical properties, and J the sensitivity matrix for the measurement, which can be obtained from the diffusion approximation or radiative transfer equation with analytical or numerical methods, e.g., the finite element method [5, 183] or Monte Carlo simulation [83].

The ill-posed inverse problem can be solved by using regularization [4, 5, 72]. Consequently, the solution can be obtained as:

$$\Delta x = \underset{\Delta x}{\arg\min} \left(\|\Delta y - J\Delta x\|^2 + \alpha \|L\Delta x\|^2 \right), \tag{2.3}$$

where the second part is a generalized Tikhonov regularization term with α being the regularization parameter and L the regularization matrix [102]. If L is the Laplace or gradient operator, α controls the smoothness of the resulting reconstruction.

As compared to fNIRS, DOT provides more accurate spatial information of Δ[HbO_2] and Δ[HbR] and reduces the partial volume and differential sensitivity effects, which complicate analysis of fNIRS signals [71]. In addition, it provides some depth resolution that facilitates the localization of brain activity [71].

2.5 fNIRS instrumentation

The fNIRS devices can be divided into three broad categories: continuous-wave, time-domain, and frequency-domain instruments [45]. Of these three categories, the continuous-wave instruments operate with the simplest principle; they measure attenuation of a constant light intensity in tissue. Due to the low cost, ease of implementation, efficient light detection, fast sampling, best instrumental signal-to-noise ratio (SNR), and small size, this design is the most common among commercial fNIRS devices (for reviews, see Refs. [56, 203]). However, instruments in this category cannot record absolute concentrations of chromophores nor the path length of the light in the tissue, which is useful in calculating concentrations of the chromophores with the modified Beer–Lambert law (Eq. 2.1) and in reconstructing the optical properties of the tissue in DOT [72]. A

subtype of instruments in this category perform spatially-resolved spectroscopy, i.e., multidistance measurements, to determine absolute ratios of the concentrations of the chromophores from which the tissue oxygen saturation can be calculated [177, 203].

The time-domain technique is based on sending picosecond-long light pulses to the probed volume and measuring the time-of-flight distribution of the light passed through the volume. This technique requires the most complex instrumentation and is thus the most costly among the three categories. Its benefit is that it can separate signal components that have most probably penetrated deep into the tissue based on time-gating the detected light [72]. In addition, time-domain recordings allow for estimating the path length of light in the probed volume based on the measurement [6, 45], as well as obtaining absolute concentrations of chromophores [203].

The optical path length can also be estimated with the frequency-domain technique. These instruments modulate light intensity at a radio frequency and measure the amplitude, phase, and average intensity of the signal detected after light propagation through the probed volume. Instruments in this category are cheaper than the time-domain systems, but they do not allow separating deep and shallow components by time-gating the signals. In contrast, they are well-suited for measurements with several source-to-detector separations, which can be used for separating superficial and cerebral components from each other (discussed more in detail in Section 2.6). The additional information recorded, as compared to the data available in a continuous-wave recording, allows for estimating absolute concentrations of the chromophores [59].

The fNIRS instrument used in this Thesis belongs to the frequency-domain category. Its operating principle is described in Section 2.7.1. Commercially available fNIRS instruments are reviewed in Refs. [56, 60, 203] and prototype instruments in Ref. [203].

2.6 Data analysis and interpretation

2.6.1 Recognizing scalp and systemic contribution

The fNIRS measurement is made through the scalp. Therefore, changes in scalp blood circulation, e.g., due to task-related stress [49, 50, 150], con-

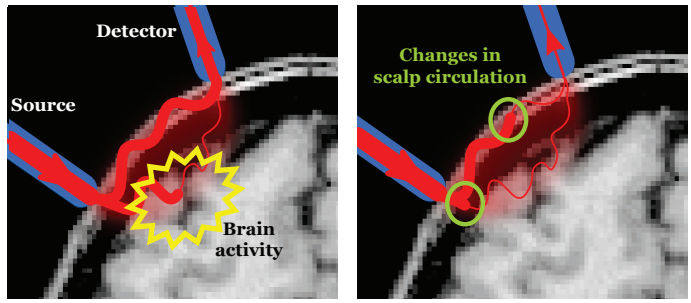

(a) Signal component related to brain activity

(b) Signal component related to superficial changes

Figure 2.2. The light travels both in the brain and superficial tissues. (a) The desired signal arises when the change in absorption occurs in response to hemodynamic changes related brain activity. (b) However, scalp circulation can also change, e.g., in response to task-related stress and alter the light absorption.

tribute to the signals (Fig. 2.2) [17, 20, 56, 67, 68, 107, 129, 178–180, 190]. Moreover, the baseline of the fNIRS signal oscillates spontaneously along with the systemic circulation, including components related to pulsation of the blood vessels, respiration, vasomotion, and autonomic regulation of the circulation [8, 17, 57, 138, 178, 189].

To distinguish other physiological components from the hemodynamic responses related to brain activity, the time evolution of the fNIRS signals can be studied; the hemodynamic responses show a characteristic waveform in event-related studies (Fig. 2.3). The hemodynamic response results from local vasodilation that increases the local CBF and raises the blood oxygenation level and volume [95]. Consequently, the increased blood volume and oxygenation manifest themselves as increased [HbO_2] and [HbT], as well as a decreased [HbR] with a smaller magnitude. The signals peak around 5 s after the stimulation onset [94, 155], and return back to the baseline with a time lag of about 5–10 s after the end of stimulation. In contrast to these hemodynamic changes, scalp and systemic components can cause other characteristics; a change in the arterial blood vessel diameter, for example, will result in Δ[HbO_2] and Δ[HbR] with the same polarity.

Besides studying the resemblance of the fNIRS signals to known characteristics of the hemodynamic responses, there is another commonly utilized method for recognizing physiological components not related to brain activity: multidistance recordings. In the simplest case, two channels with different source-to-detector separations probing approximately the same volume can be used for inferring the source of the recorded signals. Dissimilar changes in the concentrations of the chromophores at channels

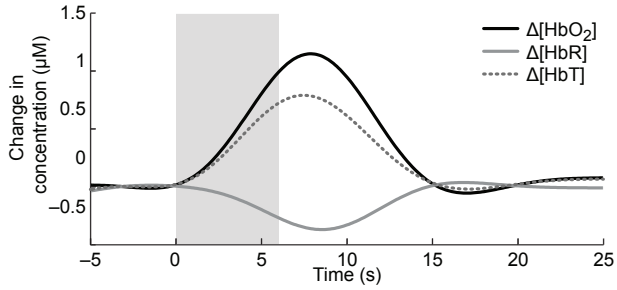

Figure 2.3. Hemodynamic response measured with fNIRS over the occipital cortex to a 6-s-long visual stimulus (gray shading). (Data from Publication I)

with a short ($<$1 cm) versus a long ($>$2.5 cm) source-to-detector separation imply distinct changes in the scalp and brain circulation. Alike changes in these channels, on the other hand, arise from either changes in scalp circulation or from parallel changes in both the brain and scalp circulation. The reasoning behind inferring the origin of the signal based on multidistance recordings follows from that the channels probe to some extent different layers of the tissue; a channel with a short separation probes the tissue shallowly whereas a channel with a longer separation records light which has penetrated deeper layers of the tissue as well [62, 70, 128, 139, 160]. Channels with a separation of 1 cm or less should almost exclusively contain superficial signals in adults [44, 128], while channels with separations larger than 2.5 cm allow for detection of cortical hemodynamic changes [44, 62, 72, 128, 139]. Signals recorded with a long source-to-detector separation, however, contain also a contribution from the superficial layers, which depends on the scalp and skull thickness [139].

In addition to the multidistance recordings, also cardiovascular parameters, e.g., heart rate and blood pressure, are helpful in setups with possible surface or systemic contribution. The cardiovascular parameters indicate changes in the systemic circulation, which may appear as scalp or systemic contribution in the fNIRS signals [46, 68, 150].

2.6.2 Removing unwanted components

To estimate and remove physiological components not related to brain activity from the fNIRS signals, several signal processing methods have been proposed in the literature. In most studies, the estimation is based on multidistance recordings, although at least one simple method can also be applied for single-channel data by assuming a specific shape for the

hemodynamic response to brain activity [205].

Superficial signal regression is a method where the superficial component is estimated from the signals with a short source-to-detector separation, fitted to and regressed from signals with a long separation [74, 159, 160, 208]. Instead of regressing the whole time series at once, in another method the signals with a long separation are filtered adaptively with the signals with a short separation [210, 211]. Furthermore, instead of using the data with a short separation directly as an estimate of the superficial contribution, the component can be estimated with principal component analysis (PCA) or independent component analysis [68, 125, 197, 212]. In many cases, the strongest principal component represents the superficial component [68, 197]. Moreover, the problem of superficial components can be approached from a different point of view: instead of estimating the physiology not related to brain activity, hemodynamic responses can be modeled with the general linear model by fitting preset hemodynamic response functions to the signals [111]. Adding heart rate and blood pressure as explanatory variables in the model gives a higher sensitivity to brain-activity-related hemodynamics [179]. Lastly, cardiovascular parameters can be included in a physiological model to predict fNIRS signal changes due to components not related to brain activity [46].

All the above-mentioned signal processing methods have the disadvantage that they assume the superficial and cerebral components to be uncorrelated or statistically independent. This is not the case in task experiments where brain activity and changes in systemic and scalp circulation occur simultaneously [20, 67, 107, 129, 179, 180, 212], causing the methods to suppress brain activity signals along with superficial components.

To avoid the issue of correlated cerebral and superficial components, some research groups have shifted from utilizing sparse fNIRS probes and analyzing data channel-by-channel to high-density recordings and DOT reconstructions [77, 108, 208]. The idea is that covering a larger area and probing the tissue with a dense probe allows for the detection of local activations more easily than with a small and sparse probe. Furthermore, DOT provides some depth discrimination [71], enabling the exclusion of surface layers from the data analysis to a certain degree [82, 108].

2.7 fNIRS methods in this Thesis

2.7.1 Instrumentation

The research constituting this Thesis was carried out with a frequency-domain instrument developed at Aalto University School of Science [133, 135]. As light sources, it uses laser diodes at two time-multiplexed wavelengths (685/756/785 and 824/830 nm). The intensity-modulated light (100 MHz) is guided into maximally 16 time-multiplexed source fibers, whose terminals are attached to the surface of the tissue. The average optical power penetrating tissue is 4–15 mW depending on the wavelength and fiber length. As the instrument time-multiplexes the source channels and wavelengths, the sampling frequency decreases as the number of active sources and wavelengths increases.

The modulation amplitude and phase shift are detected with up to 16 photomultiplier tubes coupled to the tissue via optical fiber bundles. The gain of the photomultiplier tubes is adjustable, allowing the instrument to measure a wide optical power range and enabling the use of several source-to-detector separations in the same recording. The possible source-to-detector separations of the instrument range from about 1 to 5 cm; the detected light intensity is low in over 5-cm channels of the instrument because most of the light has been absorbed, causing these channels to be usually too noisy for detecting physiological signals in adults.

The instrument has two types of fiber terminals: straight terminals and prism terminals. The straight terminals are better suited when measuring over hair because hair can be moved away from under the fiber holders with pressurized air. Hair between the fiber terminal and scalp surfaces causes coupling errors to the data [165]. On the other hand, when access close to the scalp is needed, e.g., by other instrumentation, prism terminals are better suited; they reflect the light in 90-degrees angle in the terminal making the fibers run parallel to the head surface and leaving more space above the fNIRS probe (thickness $<$1 cm) [197]. Furthermore, the effect of movement-related artifacts is smaller with the prism terminals. The activation measurements of Publication I were performed with straight terminals to reduce the contribution of coupling errors. To reduce movement artifacts, prism terminals were selected for the sleep measurements of Publications II–III and the task-activation measurements on the forehead of Publication V. They were also used to facilitate the simul-

taneous TMS of Publication IV, which requires access close to the head surface.

Besides fiber terminals, also the measurement probe can be customized. A simple probe with only one source has a higher temporal resolution and a better SNR than a probe with more sources, which, in contrast, provides a better spatial resolution and enough data for DOT reconstructions. Simple configurations with one to four sources were utilized in the measurements of Publications I, II, III, and IV, whereas the recordings of Publication V were performed with a high-density multidistance probe with 15 sources and 15 detectors to allow DOT.

2.7.2 Signal processing

The raw data of the instrument used in this Thesis includes the attenuation of the modulation amplitude and the phase shift. Before further analysis, these signals are resampled. This serves for two purposes: to obtain an even sampling rate, as the sampling rate of the data collection is not exactly a constant, and to interpolate the data of separate wavelengths and sources to have the same time vector, as the sources and wavelengths are time-multiplexed. The attenuation of the modulation amplitude is usually detrended to minimize instrumental drift and low-pass filtered to reduce high-frequency noise arising in the instrument. The phase signals are calibrated to allow estimating the optical path length [135, 182]. The signals are converted to $\Delta[HbO_2]$ and $\Delta[HbR]$ with the modified Beer–Lambert law (Eq. 2.1) either utilizing the estimated path length (Publications I–III) or a literature value for DPF (Publications IV and V) [51, 195]. After this, $\Delta[HbO_2]$ and $\Delta[HbR]$ are filtered, if wanted, to reduce physiological noise, such as cardiac oscillations [57]. In event-related studies, the signals are divided into epochs time-locked to stimuli or events, baseline-corrected, and averaged.

2.7.3 Contribution of scalp and systemic circulation

In the event-related studies of this Thesis, interstimulus intervals were randomized to avoid spontaneous physiological fluctuations synchronizing to the stimuli. Moreover, in Publication IV, the head of the subjects was lowered so that the recording was performed in a half-sitting position, as a supine position reduces the amplitude of these fluctuations [178]. To reduce the contribution of superficial components in the fNIRS signals,

the measurement probe was pressed tightly against the scalp in all studies of this Thesis [180]. Furthermore, heart rate was monitored to indicate changes in the systemic circulation. To show signals with different contributions from scalp and brain layers, all publications of this Thesis present signals from channels with short and long source-to-detector separations or DOT reconstructions.

Superficial signal regression was tested for the data of Publications IV and V and the general linear model for the data of Publications I and IV. Simple PCA filtering was applied to the data of Publication II. However, the suitability of these methods for the studies was unclear, as the brain activity seemed to correlate with other physiological components, and thus the publications present mainly results from the unprocessed data.

3. Combining fNIRS with other modalities

3.1 Chapter overview

This chapter describes the modalities that were combined with fNIRS in this work. Each section provides a general overview of the corresponding modality and reviews literature on simultaneous measurements with fNIRS. Each section also compares these concurrent measurements to similar multimodal setups with positron emission tomography (PET) and fMRI (except for cardiovascular parameters). Moreover, the sections explain how the methods of interest were used in the studies of this Thesis. Table 3.1 at the end of this chapter summarizes the advantages and disadvantages of fNIRS in multimodal setups as compared to fMRI and PET.

3.2 Electroencephalography (EEG)

Publication I presents a study on combining fNIRS with EEG. EEG is the noninvasive recording of electrical brain activity with electrodes attached on the scalp surface [11]. It is sensitive to electric fields generated mainly by synchronized postsynaptic activity in groups of neurons. It can record spontaneous brain activity, which is of interest, e.g., in connectivity studies, as well as evoked potentials, which arise in response to a stimulus.

When combined with fNIRS, EEG has many applications. Simultaneous EEG/fNIRS can give insight into physiological mechanisms that are difficult to study with only one modality [54]. On the other hand, simultaneously recorded EEG data can be used to explain fNIRS results [84, 89, 106, 209] and to verify that subjects are following the task requirements during the measurement [93]. Moreover, fNIRS data can serve as a prior in the inverse problem of EEG, which is ill-posed [1].

The combined measurement can be also applied for studying neurovascular coupling. As the two methods measure different aspects of brain activity, namely the electrical and the vascular (for review, see Ref. [155]), the combined measurement can serve in investigating how these two aspects are related [91, 109, 110, 137, 157, 181, 209] (for review, see Ref. [167]). This was also the aim of Publication I. This field of research is important because in functional hemodynamic imaging it is often assumed that hemodynamic responses are linearly and time-invariantly dependent on the underlying neuronal activity [31]. However, this might not always be the case; the location of the strongest change in blood oxygenation and CBF might not match the location of the strongest neuronal activity [32], or the magnitude of the hemodynamic response may not follow a strict linear relationship with the underlying neuronal activity [110].

The combination EEG/fNIRS is a compelling alternative to the simultaneous measurement of EEG and PET or fMRI (Table 3.1). PET exposes the subjects to radiation and has a low temporal resolution, whereas fNIRS is safe and has a higher temporal resolution. Simultaneous EEG/-fMRI is technically complicated, requires special hardware and software, and has a lower SNR than when the two modalities are used separately [27–30]. In contrast, EEG/fNIRS can be recorded basically without any modifications to the instruments and without reductions in the SNR. In addition, it tolerates movement better than EEG/fMRI [196] and is silent. As compared to fMRI and PET, fNIRS has, however, a more modest spatial resolution and can only measure changes occurring in the superficial parts of the brain. A minor technical challenge in combining EEG and fNIRS is the integration of electrodes and optodes. For measuring the data of Publication I, the fNIRS optodes were attached to an existing EEG cap. Some other studies have implemented integrated opto-electrodes for measuring fNIRS and EEG exactly in the same locations [37, 109, 199].

3.3 Polysomnography (PSG)

Publications II and III present simultaneous fNIRS and PSG. PSG is multiparametric monitoring of sleep and includes the recording of spontaneous neuronal brain activity with EEG, eye movements with electrooculography (EOG), muscle activity with electromyography (EMG), and heart rate with electrocardiography (ECG) [145]. Furthermore, arterial oxygen saturation (SpO_2), respiration, and movements are monitored often as

well.

Based on the PSG, neurophysiologists score sleep into stages N1–N3 and rapid-eye-movement sleep (REM) [96]. Stages N1–N2 represent light sleep, where the awareness of the surrounding environment disappears. N3 is the deepest stage, and it is often referred to as slow-wave sleep [170]. REM is mostly associated with dreaming, albeit dreaming also occurs in non-REM stages [123]. Non-REM and REM periods alternate four to six times during a typical night [104]. In addition to this characteristic cyclic variation of brain activity, there is also variation within each sleep stage. The phasic alteration of background activity and transient events (2–60 s) in the EEG within non-REM stages is called cyclic alternating pattern (CAP) (for reviews, see Refs. [144, 184] and for scoring rules Ref. [185]). It is thought to be related to sleep instability and preservation [144], as well as consolidation of learning [3, 61], and even creativity [47].

Research based on PSG is well established [170]. In contrast, cerebral hemodynamics has been less intensively assessed during sleep. Most studies on hemodynamics of sleep have utilized PET in combination with PSG, although PET exhibits some limitations (Table 3.1): It cannot be applied for monitoring but rather just for recording after a specific sleep stage has been reached [124]. Furthermore, it cannot capture the evolution of hemodynamics during fast events (in the order of seconds) because its temporal resolution is in the order of a minute [43]. The application of fMRI, on the other hand, is restricted by the noisy environment, technical difficulty of combining PSG with fMRI [52], and traditional fMRI signal analysis methods (general linear model) that are not optimally suited for sleep studies [43, 52]. Nevertheless, as the field of connectivity research is getting more established, connectivity analysis has been applied in fMRI sleep studies [88, 119, 161, 175]. In contrast to PET and fMRI, fNIRS is well suited for monitoring sleep with concurrent PSG and has thus been utilized in some adult sleep studies [48, 92, 97, 118, 151, 168, 174, 191]. Its major drawbacks compared to PET and fMRI are the low spatial resolution and the restricted sensitivity to only cortical activity. On the other hand, it can tolerate small movements [196], its temporal resolution is superior and it can be used for overnight monitoring. These characteristics make fNIRS especially suitable for tracking relatively fast hemodynamic changes in overnight recordings, e.g., transient events of CAP cycles (Publication III), transitions between sleep stages (Publication II), and slow hemodynamic oscillations (Publications II and III).

Previous fNIRS studies have associated the wakefulness–sleep transition with decreasing [HbO_2] in the prefrontal cortex [92, 118, 168, 174] and the opposite transition with increasing [HbO_2] [92, 118, 174], possibly reflecting the reduced complexity of brain activity during sleep. The changes in [HbR] have not been as consistent; it has been reported both to increase [92, 118, 168] and to decrease [118, 174] when falling asleep. In addition to the transition from asleep to awake, [HbO_2] has also been reported to increase in the prefrontal cortex in the transition to REM [118], probably in response to dreaming. Other studies focusing on dreaming have shown that REM activates the visual cortex [97] and lucid dreaming of a motor task the sensorimotor cortex [48]. Besides research on healthy subjects, patients with sleep disorders have also been studied with fNIRS, indicating that sleep-disordered breathing, as well as periodic leg movements in sleep, alter cerebral hemodynamics [80, 127, 141, 152–154, 194, 198]. Furthermore, sleeping infants have been studied with PSG/fNIRS [115, 116, 156].

The results of fNIRS research are generally in line with PET studies that have reported global and a local prefrontal decrease in the CBF, corresponding to a lowered [HbO_2], in non-REM as compared to wakefulness [41, 43]. In REM, the global CBF is comparable to wakefulness, although the prefrontal CBF has been observed to decrease as compared to wakefulness [43].

In most of the fNIRS studies, subjects have been measured during daytime napping; only two studies published before Publication II have investigated full-night recordings [92, 168]. As a consequence, slow-wave sleep has been mostly neglected, albeit one study reports decreasing [HbO_2] with the sleep getting deeper [92]. The aim of Publication II was to study slow-wave sleep, focusing on differences between slow-wave and light sleep. Moreover, Publication II characterizes transitions between sleep stages.

The temporal resolution of PET hinders the direct study of CAP-related activity. By contrast, fNIRS can record hemodynamics of CAP whose prevalence is elevated in various sleep disorders [144]. Publication III reports the first systematic study on hemodynamics during CAP in healthy subjects; previous fMRI and PET studies characterize CBF changes during specific CAP events [40, 42, 43] and one fNIRS study during periodic leg movements [153].

Low- and very-low-frequency oscillations (0.04–0.15 and 0.003–0.04 Hz,

respectively) constitute a considerable proportion of physiological variation in fNIRS signals [57, 93, 138, 188] (for review, see Ref. [162]). These oscillations have been attributed to many underlying factors, such as neuronal activity [63, 87, 91, 103, 202], vasomotion [57], and autonomic control of the systemic circulation [68, 103, 178], and they are clearly visible in sleeping subjects as well. Publications II and III are among the first fNIRS studies to investigate these oscillations in sleeping adults. The oscillations have also been studied in sleeping infants [156] and recently in sleeping adults in a study investigating the phase difference between $\Delta[HbO_2]$ and $\Delta[HbR]$ [151].

3.4 Transcranial magnetic stimulation (TMS)

Publication IV reports a study combining fNIRS with TMS, which is a method for activating the brain in a direct and controlled manner [9]. It is based on a rapidly changing localized magnetic field that produces an electric field in the tissue which in turn excites and inhibits neuronal activity [98]. If a specific brain area is stimulated, the effect of TMS can sometimes be observed, e.g., as a finger movement or as a short-term inability to produce speech [9, 146]. On the other hand, longer-lasting treatment effects have been seen in patients who have received TMS therapy. The therapy constitutes of intensive stimulation sessions repeated many times per week to treat depression, to rehabilitate brain areas affected by stroke, etc. (for reviews, see, e.g., Refs. [143, 163, 164, 201]).

TMS does not always produce a noticeable change in the subject's behavior. This does not mean that the stimulation does not activate neurons—the effect just cannot be observed directly in the behavior. To assess the TMS-evoked brain activity in a more direct manner and to facilitate the study of TMS-evoked activity in these kinds of situations, it has been combined with several functional neuroimaging methods.

The neuronal activity evoked by TMS can be recorded with TMS-compatible EEG devices [99]. TMS/EEG studies have demonstrated that even a low-intensity stimulation (below motor threshold) evokes recordable brain activity [112, 113]. Studies have also illustrated how the TMS-evoked local activation spreads in the brain to connected areas [99] and how this spreading is suppressed in sleep [126]. However, not all brain areas can be easily studied with TMS/EEG, as the stimulation of cranial muscles causes strong artifacts in EEG, masking brain activity [114, 121].

TMS has also been combined with hemodynamic modalities (PET, fMRI, and fNIRS) to record the hemodynamic counterpart of the TMS-evoked brain activity [21, 64, 140, 148] (for reviews, see Refs. [15, 147]). These studies have mainly investigated the effect of several repeated TMS pulses (repetitive TMS) on the hemodynamics of the brain. However, the results have been variable depending on the method and TMS parameters. PET studies with sub- and suprathreshold repetitive TMS have mostly reported an increase in the local CBF, corresponding to a [HbO_2] increase and [HbR] decrease, on the stimulated motor cortex [64, 66, 169, 172] and occipital cortex [148], although decreases have also been observed on the stimulated motor [149] and prefrontal cortices [173]. On the contralateral motor cortex, CBF has been reported to decrease following sub- and suprathreshold stimulation [64, 66].

Most fMRI studies are in line with PET studies: the blood-oxygen-level-dependent signal (BOLD), which is inversely correlated with [HbR], has been reported to increase on the stimulated motor cortex following suprathreshold stimulation [10, 13, 14, 22, 24–26, 105] and decrease on the contralateral cortex [13, 14, 105]. Unlike PET studies, fMRI studies report no changes in the stimulated motor cortex when subthreshold intensities are applied [10, 13, 14]. This may be because susceptibility artifacts reduce the contrast in tissue areas directly below the TMS coil [23].

In contrast to the majority of PET and fMRI studies, fNIRS studies report mostly decreased [HbO_2] on stimulated motor [75, 78, 117] and prefrontal cortices [2, 117, 187] as well as on the contralateral motor [85, 100, 117, 130] and prefrontal cortices [79, 117, 130] with sub- and suprathreshold intensities. Nonetheless, one study has reported increased [HbO_2] on the stimulated motor cortex following suprathreshold TMS [140]. The results regarding [HbR] have mainly been statistically insignificant or not reported. Single TMS pulses have been reported to both increase [HbO_2] [136] and to decrease [HbO_2] and [HbT] in the stimulated area [131, 186]. Publication IV explains the discrepancy between the results from fNIRS and other methods as physiological artifacts in fNIRS signals in response to TMS.

Besides measuring TMS-evoked brain activity, the effect of TMS can also be evaluated as increased or reduced performance to a specific task. These aftereffects of repeated TMS also affect the hemodynamics of the brain, as shown in some fNIRS studies [36, 58, 206]. However, suitable tasks for studying the aftereffects often include mental or physical effort,

which may add scalp contribution to the fNIRS signals. Scalp circulation was studied in Publication V in order to develop a viable method for recording the aftereffects of TMS therapy.

3.5 Cardiovascular parameters

Cardiovascular parameters were monitored in all studies of this Thesis to evaluate various aspects of the systemic circulation. These parameters are important since they serve as indicators for possible scalp or systemic contribution in fNIRS signals. Despite their importance and ease of measurement, they are not regularly reported in fNIRS studies. Nevertheless, in studies specifically investigating the scalp and systemic contribution in fNIRS, heart-rate [67, 107, 179], blood-pressure [107, 129, 179], and scalp blood-flow changes have been recorded [107, 179, 180].

In this Thesis, heart rate was obtained mainly from the photoplethysmogram (PPG) recorded with a pulse oximeter, which also measures SpO_2 (Publications II and III). PPG reflects the state of the circulation and the amplitude of the PPG waveform (PPGamp) provides a measure of the volume of blood pulsating in the blood vessels of a finger tip. PPGamp depends on the local vascular compliance [166] and decreases with vasoconstriction as a consequence of a stress reaction. Moreover, it is affected by the systemic vascular tone. PPGamp is presented in Publications II, III, and IV.

Pulse transit time (PTT) is a cardiovascular parameter, which can be assessed from a simultaneous PPG and ECG recording (Publication IV). It represents the time taken by a pressure wave resulting from a heartbeat to travel from the heart to the finger tip. It characterizes arterial stiffness along the path that the pressure wave travels, and its inverse is correlated with blood pressure [132]. Furthermore, it depends on the systemic vascular tone.

Table 3.1. Comparison of hemodynamic modalities in multimodal setups.

	fNIRS	fMRI	PET
Parameters	$\Delta[HbO_2]$, $\Delta[HbR]$, $\Delta[HbT]$	BOLD	CBF or glucose metabolism
Setup	natural environment	shielded room	shielded room
Monitoring	yes	no	no
Temporal resolution	best ($<$1 s)	intermediate (~1 s)	worst ($>$1 min)
Spatial resolution	worst (~1 cm)	best (~1 mm)	intermediate (~5 mm)
Sensitive to subcortical areas	no	yes	yes
Sensitivity to movement	moderate	high	high
Safety issues in general	–	projectile effects; noise	radioactive tracers
with EEG	–	electrode and wire heating	–
with TMS	–	projectile stimulator unit	–
Technical issues with EEG	–	strong artifacts in EEG	–
with TMS	fNIRS probe has to be thin	nonferromagnetic TMS coil; customized fMRI coil; susceptibility and other artifacts in fMRI	detector shielding
Limitations with EEG	scalp and systemic contribution	technical (low SNR of EEG)	time scales different
with TMS	physiological artifacts	technical (low SNR of fMRI)	temporal resolution
during sleep	scalp and systemic contribution	noise and movement restrictions; technical	measurement can be performed every ~30 min

4. Summary of publications

4.1 Chapter overview

This chapter summarizes the main results of the publications constituting this Thesis. Details on the data analysis can be found in the publications.

4.2 Publication I: Combining EEG and fNIRS in awake subjects

Publication I describes a study on awake subjects combining EEG and fNIRS. The aim was to prove the feasibility of the simultaneous recordings with the instruments available at Aalto University. Furthermore, Publication I demonstrates that a combined EEG/fNIRS setup can be applied for studying the relationship between hemodynamic and neuronal brain activity on which hemodynamic imaging with fNIRS, fMRI, and PET is based on.

In the study, pattern-reversing checkerboard stimuli of different durations (3, 6, and 12 s) produced hemodynamic responses recordable with fNIRS, with the area-under-curve of the responses increasing along with the stimulus duration (Fig. 4.1). The simultaneously recorded EEG-based visually-evoked potentials, representing a measure of neuronal activity, correlated linearly with area-under-curve of the hemodynamic responses (Fig. 4.1b), indicating a linear relationship between neuronal activity and hemodynamic responses on the occipital cortex with the applied stimuli.

The direct brain-activity-derived measure (visually-evoked potentials) had a higher correlation with the fNIRS responses than the stimulus duration (Fig. 4.1b), suggesting that the observed fNIRS responses reflected brain activity rather than other effects, such as changes in scalp circulation. Moreover, no large changes in the heart rate were observed during

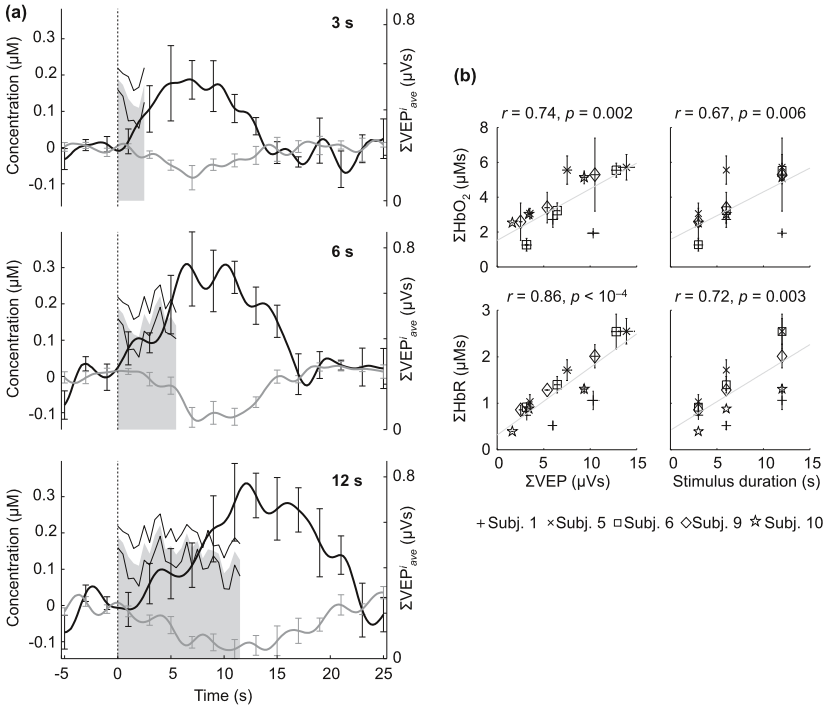

Figure 4.1. (a) Δ[HbO$_2$] (black line) and Δ[HbR] (gray line) responses in the occipital cortex to 3-s-, 6-s-, and 12-s-long flickering checkerboard stimuli (beginning at 0 s) and simultaneous area-under-curve of visually-evoked potentials recorded with EEG (ΣVEP$^i_{ave}$; gray shaded area). Error bars and thin black lines indicate the standard error of the mean. (b) Area-under-curve of Δ[HbO$_2$] and Δ[HbR] (ΣHbO$_2$ and ΣHbR) as a function of ΣVEP$^i_{ave}$ integrated over the stimulus duration (ΣVEP) and as a function of the stimulus duration. Pearson's correlation coefficients (r) and their statistical significance (p) are marked above each scatter plot. (Modified from Publication I)

the recordings, suggesting that the protocol did not likely affect the systemic circulation. In addition, the amplitudes of the responses were larger in channels with a long source-to-detector separation (4 cm) than in the shorter ones (2 cm) and more often statistically significant. Furthermore, the shape of the responses corresponded to the expected one [94].

4.3 Publications II & III: Monitoring sleep with PSG/fNIRS

Publications II and III describe a study combining PSG and fNIRS in healthy sleeping subjects, providing an approach for investigating hemodynamics of sleep-stage transitions, hemodynamic markers of unstable sleep, and characteristics of low-frequency oscillations in sleep.

Publication II reports the first systematic fNIRS study on transitions between sleep stages incorporating slow-wave sleep. The publication demonstrates that hemodynamic changes in these transitions are asymmetric:

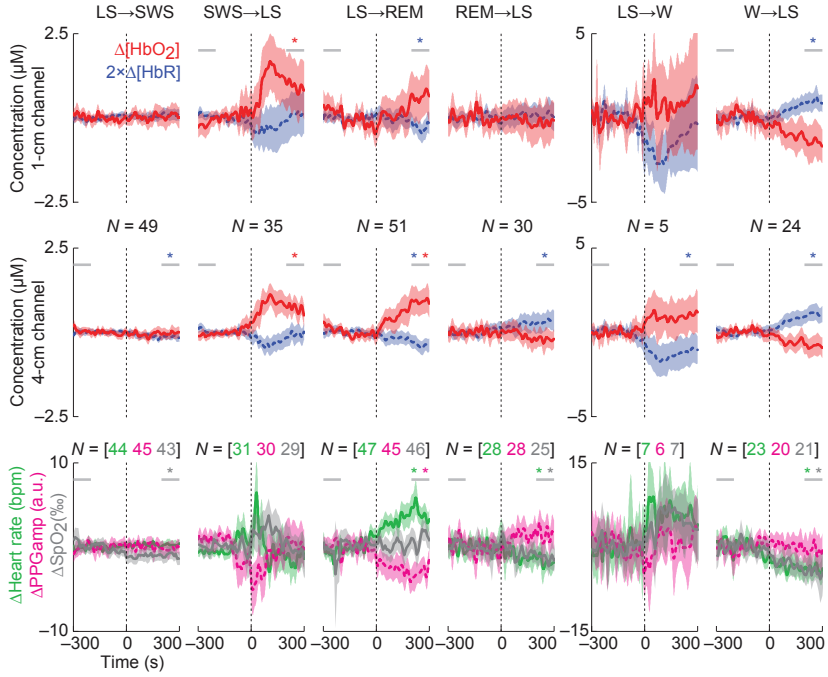

Figure 4.2. $\Delta[HbO_2]$ and $\Delta[HbR]$ on the forehead and cardiovascular parameters in transitions between sleep stages (LS: light sleep, SWS: slow-wave sleep, W: wakefulness). The dotted vertical line depicts the transition and shading the 95% confidence interval. N is the total number of transitions averaged. Asterisks mark significant changes in signal levels from $-300\ldots-200$ to $200\ldots300$ s (paired t-tests). (Modified from Publication II)

transitions associated with an increase in brain electrophysiological activity (from slow-wave sleep to light sleep and from light sleep to REM) were related to more dramatic hemodynamic changes than the opposite transitions in the study (Fig. 4.2). Thus, transitions involving a reduction in cortical electrical activity, indicating a transition to a deeper sleep stage or drifting away from REM, appear as gradual processes over time, whereas the increase in electrical cortical activity, marking a transition to a lighter sleep stage or to REM, may be triggered more abruptly by a particular physiological event or condition.

Publication III focuses on CAP, which is a microstructure of non-REM and related to sleep instability. It describes the first fNIRS study on hemodynamics of unstable sleep in healthy subjects. The results presented in the publication demonstrate that, in addition to hemodynamic changes related to transitions between sleep stages, also the microstructure of sleep is reflected in the scalp, cerebral, and systemic hemodynamics (Fig. 4.3). The hemodynamic changes during CAP reported in this publication resemble the ones observed during arousal caused by sleep-disordered breathing in another study [198], thus underlining the impor-

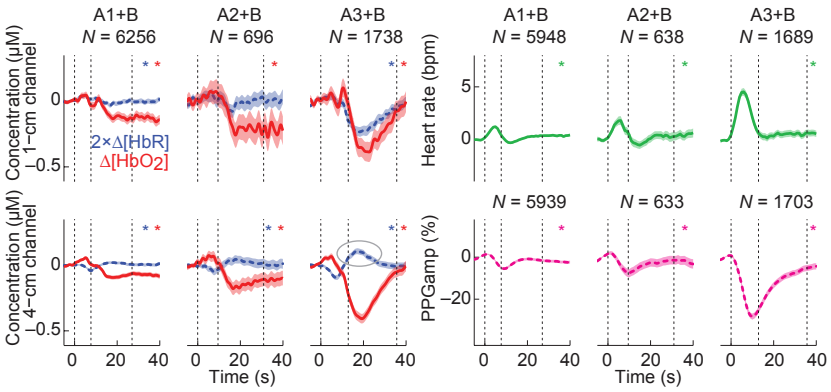

Figure 4.3. Hemodynamic signals in subtypes A1+B, A2+B, and A3+B of CAP. Shading depicts the 95% confidence interval of the mean and vertical lines the beginning of phase A (0 s), the average beginning of phase B (~10 s), and the average end of phase B (~30 s). *N* is the number of cycles averaged and asterisks indicate statistically significant signals (one-way analysis of variance). The gray ellipse marks a hypoxic period. (Modified from Publication III)

tance of autonomic regulation in situations with a potential for arousal (sleep instability). Furthermore, the results indicate a transient hypoxia during CAP (Fig. 4.3), which may cause harmful effects in the vasculature [12]. The hypoxia may explain the link between the increased risk for cardiovascular diseases in patients with sleep disorders and their elevated CAP rates [73, 144].

Publications II and III present the first fNIRS studies reporting low- and very-low-frequency hemodynamic oscillations in sleeping healthy adults. Publication II demonstrates that these oscillations are weaker in slow-wave sleep than in light sleep, REM, and wakefulness (Fig. 4.4a). The suppressed amplitude of these oscillations during non-REM as compared to wakefulness and REM has been confirmed later on by another fNIRS study [151]. Publication III shows that CAP sequences, which are repetitive by nature, are related to hemodynamic oscillations at low and very-low frequencies (Fig. 4.4b). The publication discusses that the suppressed amplitude of the oscillations in slow-wave sleep may partly be attributed to the rarity of the subtype A3 of CAP in this sleep stage (3% vs. 20% of total time in light sleep): this subtype causes the strongest hemodynamic changes (Fig. 4.3) and thus strongest CAP-related hemodynamic oscillations (Fig. 4.4b).

Publications II and III report mostly simultaneous changes in fNIRS signals and cardiovascular parameters (heart rate, PPGamp). Therefore, it is not fully clear if the recorded fNIRS signals represent scalp, systemic, or cerebral hemodynamics—probably a combination of all of these. Nevertheless, by observing signals from separate channels, it is possible

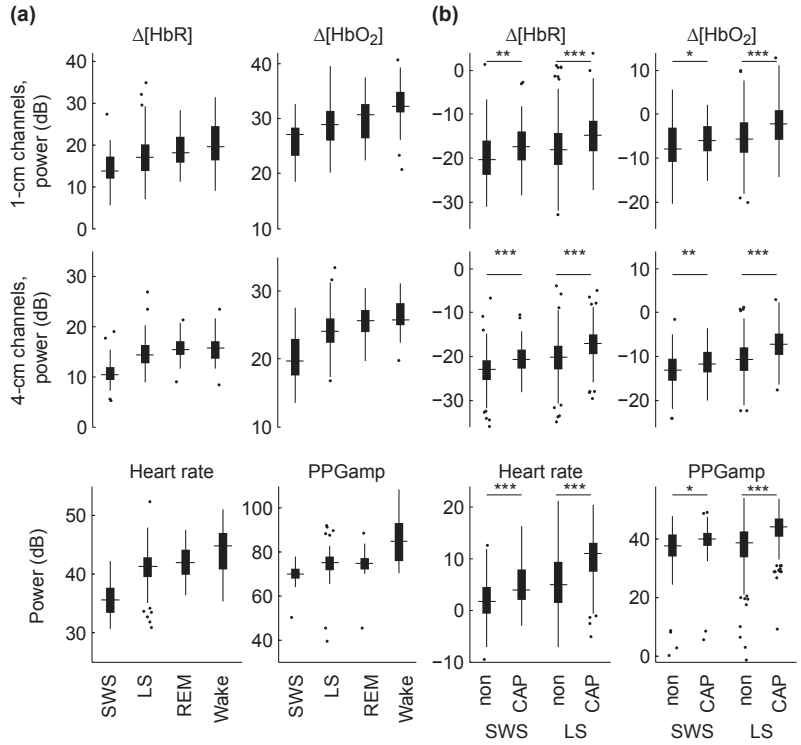

Figure 4.4. Oscillatory power of combined low- and very-low-frequency oscillations in hemodynamic signals (a) in separate sleep stages (SWS: slow-wave sleep, LS: light sleep, W: wakefulness) and (b) during CAP vs. non-CAP periods separately in slow-wave and light sleep. The data in (a) are presented as power/Hz and in (b) as total power in the frequency range which causes the y-axis to differ between (a) and (b). Asterisks and horizontal bars indicate significant differences (t-tests). (Modified from Publications II and III)

to deduct changes related to brain activity from the data of Publication III: the polarity of Δ[HbR] responses changes from the 1-cm to the 4-cm channel, indicating decreased blood oxygenation in the brain during CAP cycles (Fig. 4.3).

4.4 Publication IV: TMS-evoked artifacts in fNIRS

Publication IV describes a study that combines fNIRS with TMS. The aim of the study was to investigate the feasibility of recording hemodynamic responses reflecting TMS-evoked brain activity with fNIRS. The fNIRS recording was technically possible on the stimulation site, as the fNIRS probe was thin enough for the magnetic pulses not to be attenuated extensively by the increased distance between the coil and brain. Despite the technical simplicity of TMS/fNIRS, the results obtained with the technique need to be interpreted with caution. Publication IV demonstrates

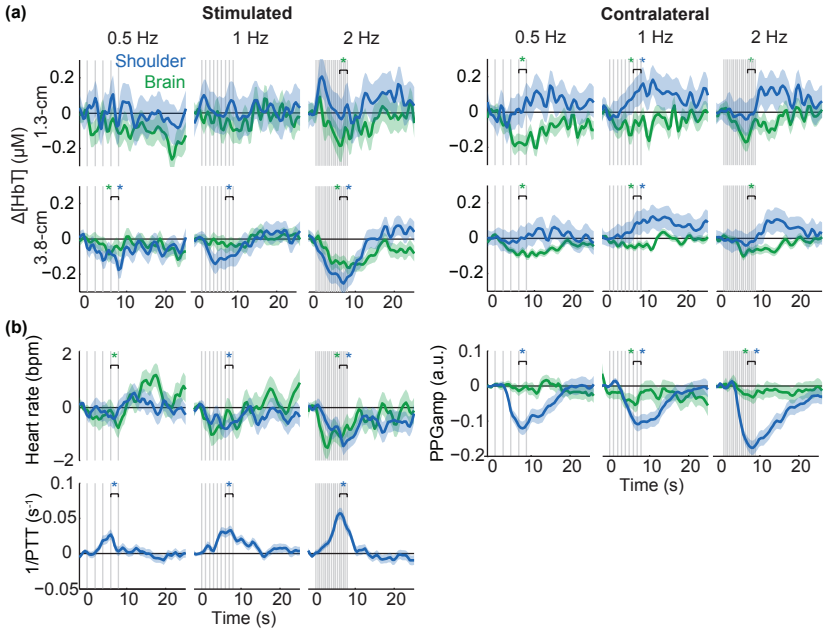

Figure 4.5. (a) Δ[HbT] responses following 0.5-, 1-, and 2-Hz repetitive TMS recorded on the stimulated and contralateral hemispheres and shoulders with 1.3-cm and 3.8-cm channels. (b) Changes in cardiovascular parameters following TMS. Shading depicts the standard error of the mean and vertical lines time instances of the magnetic pulses. Asterisks indicate responses with statistically significant average amplitudes at the end of the magnetic pulse train as compared to the baseline (paired *t*-tests). (Modified from Publication IV)

that TMS-evoked fNIRS signals contain physiological artifacts not related to TMS-evoked brain activity.

The publication compares Δ[HbT] responses on the stimulated and contralateral motor cortex with responses measured on the shoulders following shoulder stimulation. The comparison reveals a close correspondence between the responses on the stimulated hemisphere and shoulder (Fig. 4.5a). Furthermore, simultaneous changes in cardiovascular parameters were observed in the study (Fig. 4.5b). As the responses on the shoulders cannot stem from hemodynamic responses to brain activity, the publication discusses the possible origin of the responses as being direct vasoconstriction produced by TMS, indirect vasoconstriction through stimulation of nerves controlling the diameter of the blood vessels, or a systemic circulatory response to the discomfort of the stimulation (Fig. 4.6). All of the mechanisms explaining the Δ[HbT] responses on the shoulders will also affect responses measured on the motor cortex following brain stimulation, inducing components to the fNIRS signals not related directly to the TMS-evoked brain activity.

Publication IV presents evidence that TMS-evoked fNIRS responses con-

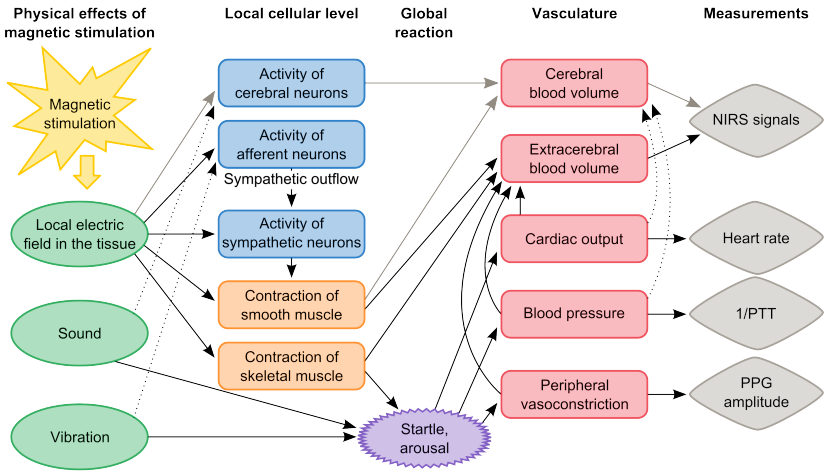

Figure 4.6. Effect of magnetic stimulation on the tissue and its relation to measured parameters. Black solid lines present relations in both brain and shoulder stimulation and gray lines only in brain stimulation. Dotted lines are not meaningful in terms of interpreting the data. (From Publication IV)

tain physiological artifacts and thus TMS/fNIRS results should be interpreted with caution. If TMS causes direct vasoconstriction in the brain, also other hemodynamic imaging modalities, including fMRI, are affected by it and are not able to record hemodynamic responses related to TMS-evoked brain activity on the stimulation site. On the other hand, if the artifact arises in the surface tissue, it should be possible to isolate brain-activity-related hemodynamic responses with signal processing methods or with DOT.

4.5 Publication V: Effect of scalp circulation on DOT

Publication V describes a study on scalp effects in event-related DOT. The publication demonstrates that changes in scalp circulation can be assessed by evaluating separately the extra- and intracranial projections of the DOT reconstructions together with the heart rate.

In the study, physically and mentally demanding tasks (hand-motor and verbal-fluency tasks, respectively) caused changes in the scalp circulation in response to task-performance-related stress and produced changes in the extracranial projections of the reconstructions (Fig. 4.7a). The changes depended on the heart rate that reflects the strength of the stress reaction (Fig. 4.7b). To understand better the effect of scalp circulation on the reconstructions, changes in scalp and brain circulation were simulated. The simulations indicated crosstalk between intra- and extracra-

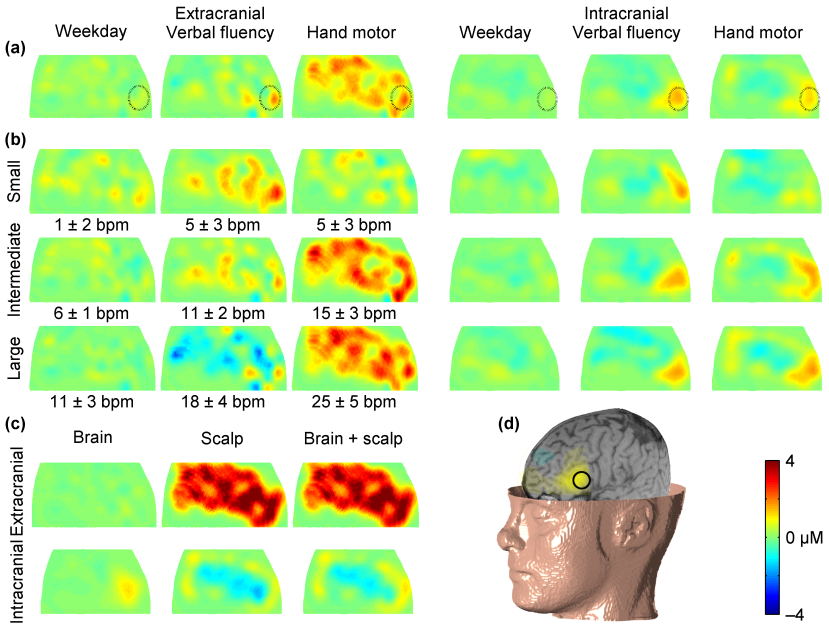

Figure 4.7. (a) Extra- and intracranial projections of reconstructed Δ[HbT] during weekday-recitation, verbal-fluency and hand-motor tasks. (b) Δ[HbT] projections in task repetitions with small, intermediate, and large changes in heart rate. (c) Δ[HbT] projections of reconstructed simulated brain activity, change in scalp circulation, and a combination of these two. (d) Intracranial Δ[HbT] projection during the verbal fluency task overlapped over the magnetic resonance image of one subject. The approximate location of the inferior frontal gyrus is depicted with a circle in (a) and (d). ((a)–(c) modified from Publication V)

nial layers of the reconstructions (Fig. 4.7c), suggesting that strong alterations in the scalp circulation can distort the brain activation images. Accordingly, the crosstalk artifact was visible in the intracranial projections during the hand-motor task, and it depended on the heart rate (Fig. 4.7a,b).

In contrast to the hand-motor task, the verbal-fluency task showed an activation in the brain compartment that was not dependent on the simultaneously occurring change in the heart rate (Fig. 4.7a,b). Furthermore, it did not resemble the crosstalk artifact. As the activation peak was located in the left inferior frontal gyrus (Fig. 4.7a,d), matching the expected location of brain activity [39, 81], it appears that the simultaneous reconstruction of hemodynamic changes in the intra- and extracranial layers, combined with the heart-rate measurement, allowed for identifying the brain-activation-dependent hemodynamic response to the verbal-fluency task. The publication discusses, however, that sophisticated instrumentation and reconstruction methods are needed to fully eliminate the crosstalk artifacts, especially when task-related stress is involved.

5. Discussion and conclusions

The research constituting this Thesis combines fNIRS with EEG, PSG, TMS, and cardiovascular recordings. It demonstrates that fNIRS is well-suited for multimodal setups which can provide valuable information unobtainable with separate methods: EEG/fNIRS can be applied to study neurovascular coupling, PSG/fNIRS reveals important features about the hemodynamics of sleep, TMS/fNIRS can characterize effects of TMS on the vasculature, and finally the cardiovascular recordings inform us about task-related stress responses, which in combination with DOT can be used for studying the contribution of scalp circulation in fNIRS recordings.

Increasing evidence indicates that fNIRS signals contain also other components than hemodynamic responses related to brain activity [17, 56, 67, 68, 107, 129, 179, 180, 190]. The results presented in this Thesis support this point of view; task-related physical and mental stress produced changes in the scalp circulation of the forehead as indicated by DOT. Furthermore, TMS caused artifacts in fNIRS signals due to stimulation-related startle and/or due to stimulation-evoked vasoconstriction. In light of these observations, it is important to acknowledge that fNIRS signals do not only represent hemodynamic responses to brain activity but arise partly through other physiological mechanisms as well.

To evaluate the presence of systemic and scalp contribution, the work presented in this Thesis suggests that cardiovascular parameters should be recorded in conjunction with fNIRS, as they indicate changes in the systemic circulation, which in turn may be reflected in the fNIRS signals. Even though these parameters can be easily measured, they are relatively rarely reported in fNIRS literature. The presented DOT reconstructions show a correspondence between a substantial change in heart rate and a change in the scalp circulation, suggesting that heart rate serves as an indicator for changes in the scalp circulation on the forehead. In addition,

the presented work introduces two other parameters (PPGamp and PTT) which have not been reported before the publications of this Thesis in the fNIRS literature. Both of these parameters seem useful in characterizing possible changes in scalp and systemic circulation, as PPGamp reflects vasoconstriction related to a stress reaction and PTT is correlated with blood pressure.

To allow for better spatial sensitivity, fNIRS research has started shifting from reporting fNIRS responses in single channels to high-density DOT studies, as some groups have shown DOT to provide in some setups sensitivity comparable to fMRI in the superficial parts of the brain [53, 77, 108, 208]. The shift from fNIRS to DOT is also supported by the results of this Thesis, especially in the case of studying the effects of TMS; DOT provides better separability between intra- and extracranial hemodynamics than fNIRS and is thus more accurate for measuring local brain activity. It could also be useful when studying neurovascular coupling, as DOT can aid in solving the electric fields generating the recorded EEG signals [1]. Sleep studies would also gain from the sensitivity of DOT, but on the other hand this would make the setup more complicated. Especially in sleep applications, a simple setup is often desired to avoid disturbing the sleep. Moreover, in clinical settings simple recordings may be preferred for easier interpretation, even if the the origin of the observations is not fully clear. Take EEG as an example; it has been used in detecting sleep stages for decades, although the functional meaning of most of the sleep-related events in EEG are still under debate [34, 69]. Taken together, in some studies fNIRS is better suited and in others DOT; the best method depends on the focus of the study.

The multimodal setups presented in this Thesis can be developed further. The EEG/fNIRS was recorded with a TMS-compatible EEG cap allowing a concurrent use of TMS, EEG, and fNIRS. If the TMS-evoked physiological artifacts observed in Publication IV can be removed with DOT or some signal processing method, a combination TMS/EEG/fNIRS would be optimal for studying the neurovascular coupling, as TMS evokes brain activity in a more controlled manner than a conventional sensory stimulus. The combination might also reveal more about the effect of TMS on the vasculature. In addition to the TMS applications, sleep measurements can also be supplemented with the multitude of parameters measured in sleep laboratories today, e.g., snoring, leg movements, breathing, and position. These parameters in combination with PSG/fNIRS would

serve especially well in studying patients with sleep disorders, as their altered hemodynamics may be linked to the elevated risk for cardiovascular diseases [12, 73]. Furthermore, the currently available wireless fNIRS technology is optimally suited for recording hemodynamics of sleep, as it makes the recordings easier to implement and more comfortable for the patients [60].

In conclusion, the research presented in this Thesis contributes to the methodology and analysis techniques for monitoring hemodynamics of sleep. Owing to the accessibility to cerebral hemodynamic parameters at bedside, ease of simultaneous recording with PSG, and meaningful results, fNIRS has attracted interest among neurophysiologists in Finland. At the moment, the method can be applied in the clinic, albeit methods are needed for separating scalp and cerebral components from each other. This challenge of scalp components is even greater in monitoring the effects of TMS. The work constituting this Thesis contributes to the growing field of research on scalp effects in fNIRS signals and shows evidence of physiological artifacts in fNIRS during TMS, as well as changes in scalp circulation during mental and physical stress. This evidence increases the understanding of the origin of the fNIRS signals and advances the usability of fNIRS in monitoring sleep and the effects of TMS.

Bibliography

[1] T. Aihara, Y. Takeda, K. Takeda, W. Yasuda, T. Sato, Y. Otaka, T. Hanakawa, M. Honda, M. Liu, M. Kawato, M.-A. Sato, and R. Osu. Cortical current source estimation from electroencephalography in combination with near-infrared spectroscopy as a hierarchical prior. *NeuroImage*, 59:4006–4021, 2012.

[2] Y. Aoyama, N. Hanaoka, M. Kameyama, M. Suda, T. Sato, M. Song, M. Fukuda, and M. Mikuni. Stimulus intensity dependence of cerebral blood volume changes in left frontal lobe by low-frequency rTMS to right frontal lobe: a near-infrared spectroscopy study. *Neurosci. Res.*, 63:47–51, 2009.

[3] D. Aricò, V. Drago, P. S. Foster, K. M. Heilman, J. Williamson, and R. Ferri. Effects of NREM sleep instability on cognitive processing. *Sleep Med.*, 11:791–798, 2010.

[4] S. R. Arridge. Optical tomography in medical imaging. *Inverse Probl.*, 15:R41–R93, 1999.

[5] S. R. Arridge. Methods in diffuse optical imaging. *Phil. Trans. R. Soc. A*, 369:4558–4576, 2011.

[6] S. R. Arridge, M. Cope, and D. T. Delpy. The theoretical basis for the determination of optical pathlengths in tissue: temporal and frequency analysis. *Phys. Med. Biol.*, 37:1531–1560, 1992.

[7] S. R. Arridge and W. R. B. Lionheart. Nonuniqueness in diffusion-based optical tomography. *Opt. Lett.*, 23:882–884, 1998.

[8] R. L. Barbour, H. L. Graber, Y. Pei, S. Zhong, and C. H. Schmitz. Optical tomographic imaging of dynamic features of dense-scattering media. *J. Opt. Soc. Am. A*, 18:3018–3036, 2001.

[9] A. T. Barker, R. Jalinous, and I. L. Freeston. Non-invasive magnetic stimulation of the human motor cortex. *Lancet*, 1:1106–1107, 1985.

[10] J. Baudewig, H. R. Siebner, S. Bestmann, F. Tergau, T. Tings, W. Paulus, and J. Frahm. Functional MRI of cortical activations induced by transcranial magnetic stimulation (TMS). *NeuroReport*, 12:3543–3548, 2001.

[11] H. Berger. Über das Elektroenkephalogramm der Menschen. *Arch. f. Psychiat.*, 87:527–570, 1929.

[12] S. Berger and L. Lavie. Endothelial progenitor cells in cardiovascular disease and hypoxia—potential implications to obstructive sleep apnea. *Transl. Res.*, 158:1–13, 2011.

[13] S. Bestmann, J. Baudewig, H. R. Siebner, J. C. Rothwell, and J. Frahm. Subthreshold high-frequency TMS of human primary motor cortex modulates interconnected frontal motor areas as detected by interleaved fMRI–TMS. *NeuroImage*, 20:1685–1696, 2003.

[14] S. Bestmann, J. Baudewig, H. R. Siebner, J. C. Rothwell, and J. Frahm. Functional MRI of the immediate impact of transcranial magnetic stimulation on cortical and subcortical motor circuits. *Eur. J. Neurosci.*, 19:1950–1962, 2004.

[15] S. Bestmann, C. Ruff, F. Blankenburg, N. Weiskopf, J. Driver, and J. Rothwell. Mapping causal interregional influences with concurrent TMS–fMRI. *Exp. Brain Res.*, 191:383–402, 2008.

[16] D. A. Boas, D. H. Brooks, E. L. Miller, C. A. DiMarzio, M. Kilmer, R. J. Gaudette, and Q. Zhang. Imaging the body with diffuse optical tomography. *IEEE Signal Proc. Mag.*, 18:57–75, 2001.

[17] D. A. Boas, A. M. Dale, and M. A. Franceschini. Diffuse optical imaging of brain activation: approaches to optimizing image sensitivity, resolution, and accuracy. *NeuroImage*, 23:S275–S288, 2004.

[18] D. A. Boas, T. Gaudette, G. Strangman, X. Cheng, J. J. Marota, and J. B. Mandeville. The accuracy of near infrared spectroscopy and imaging during focal changes in cerebral hemodynamics. *NeuroImage*, 13:76–90, 2001.

[19] D. A. Boas, G. Strangman, J. P. Culver, R. D. Hoge, G. Jasdzewski, R. A. Poldrack, B. R. Rosen, and J. B. Mandeville. Can the cerebral metabolic rate of oxygen be estimated with near-infrared spectroscopy? *Phys. Med. Biol.*, 48:2405–2418, 2003.

[20] S. Boden, H. Obrig, C. Köhncke, H. Benav, S. Koch, and J. Steinbrink. The oxygenation response to functional stimulation: is there a physiological meaning to the lag between parameters? *NeuroImage*, 36:100–107, 2007.

[21] D. E. Bohning, A. P. Pecheny, C. M. Epstein, A. M. Speer, D. J. Vincent, W. Dannels, and M. S. George. Mapping transcranial magnetic stimulation (TMS) fields in vivo with MRI. *NeuroReport*, 8:2535–2538, 1997.

[22] D. E. Bohning, A. Shastri, M. P. Lomarev, J. P. Lorberbaum, Z. Nahas, and M. S. George. BOLD–fMRI response vs.transcranial magnetic stimulation (TMS) pulse-train length: testing for linearity. *J. Magn. Reson. Imaging*, 17:279–290, 2003.

[23] D. E. Bohning, A. Shastri, K. A. McConnell, Z. Nahas, J. P. Lorberbaum, D. R. Roberts, C. Teneback, D. J. Vincent, and M. S. George. A combined TMS/fMRI study of intensity-dependent TMS over motor cortex. *Biol. Psychiatry*, 45:385–394, 1999.

[24] D. E. Bohning, A. Shastri, L. McGavin, K. A. McConnell, Z. Nahas, J. P. Lorberbaum, D. R. Roberts, and M. S. George. Motor cortex brain activity induced by 1-Hz transcranial magnetic stimulation is similar in location

and level to that for volitional movement. *Invest. Radiol.*, 35:676–683, 2000.

[25] D. E. Bohning, A. Shastri, Z. Nahas, J. P. Lorberbaum, S. W. Andersen, W. R. Dannels, E. U. Haxthausen, D. J. Vincent, and M. S. George. Echo-planar BOLD fMRI of brain activation induced by concurrent transcranial magnetic stimulation. *Invest. Radiol.*, 33:336–340, 1998.

[26] D. E. Bohning, A. Shastri, E. M. Wassermann, U. Ziemann, J. P. Lorberbaum, Z. Nahas, M. P. Lomarev, and M. S. George. BOLD-fMRI response to single-pulse transcranial magnetic stimulation (TMS). *J. Magn. Reson. Imaging*, 11:569–574, 2000.

[27] G. Bonmassar, K. Anami, J. Ives, and J. W. Belliveau. Visual evoked potential (VEP) measured by simultaneous 64-channel EEG and 3T fMRI. *NeuroReport*, 10:1893–1897, 1999.

[28] G. Bonmassar, N. Hadjikhani, J. R. Ives, D. Hinton, and J. W. Belliveau. Influence of EEG electrodes on the BOLD fMRI signal. *Hum. Brain Mapp.*, 14:108–115, 2001.

[29] G. Bonmassar, P. L. Purdon, I. P. Jääskeläinen, K. Chiappa, V. Solo, E. N. Brown, and J. W. Belliveau. Motion and ballistocardiogram artifact removal for interleaved recording of EEG and EPs during MRI. *NeuroImage*, 16:1127–1141, 2002.

[30] G. Bonmassar, D. P. Schwartz, A. K. Liu, K. K. Kwong, A. M. Dale, and J. W. Belliveau. Spatiotemporal brain imaging of visual-evoked activity using interleaved EEG and fMRI recordings. *NeuroImage*, 13:1035–1043, 2001.

[31] G. M. Boynton, S. A. Engel, G. H. Glover, and D. J. Heeger. Linear systems analysis of functional magnetic resonance imaging in human V1. *J. Neurosci.*, 16:4207–4221, 1996.

[32] R. B. Buxton. The elusive initial dip. *NeuroImage*, 13:953–958, 2001.

[33] R. B. Buxton, E. C. Wong, and L. R. Frank. Dynamics of blood flow and oxygenation changes during brain activation: the balloon model. *Magn. Reson. Med.*, 39:855–864, 1998.

[34] S. S. Cash, E. Halgren, N. Dehghani, A. O. Rossetti, T. Thesen, C. Wang, O. Devinsky, R. Kuzniecky, W. Doyle, J. R. Madsen, E. Bromfield, L. Eröss, P. Halász, G. Karmos, R. Csercsa, L. Wittner, and I. Ulbert. The human K-complex represents an isolated cortical down-state. *Science*, 324:1084–1087, 2009.

[35] B. Chance, E. Anday, S. Nioka, S. Zhou, L. Hong, K. Worden, C. Li, T. Murray, Y. Ovetsky, D. Pidikiti, and R. Thomas. A novel method for fast imaging of brain function, non-invasively, with light. *Opt. Express*, 2:411–423, 1998.

[36] T.-C. Chiang, T. Vaithianathan, T. Leung, M. Lavidor, V. Walsh, and D. T. Delpy. Elevated haemoglobin levels in the motor cortex following 1 Hz transcranial magnetic stimulation: a preliminary study. *Exp. Brain Res.*, 181:555–560, 2007.

[37] R. J. Cooper, N. L. Everdell, L. C. Enfield, A. P. Gibson, A. Worley, and J. C. Hebden. Design and evaluation of a probe for simultaneous EEG and near-infrared imaging of cortical activation. *Phys. Med. Biol.*, 54:2093–2102, 2009.

[38] M. Cope. *The application of near infrared spectroscopy to non invasive monitoring of cerebral oxygenation of the newborn infant*. PhD dissertation, University College London, Department of Medical Physics and Bioengineering, 1991.

[39] S. G. Costafreda, C. H. Y. Fu, L. Lee, B. Everitt, M. J. Brammer, and A. S. David. A systematic review and quantitative appraisal of fMRI studies of verbal fluency: role of the left inferior frontal gyrus. *Hum. Brain Mapp.*, 27:799–810, 2006.

[40] M. Czisch, R. Wehrle, C. Kaufmann, T. C. Wetter, F. Holsboer, T. Pollmächer, and D. P. Auer. Functional MRI during sleep: BOLD signal decreases and their electrophysiological correlates. *Eur. J. Neurosci.*, 20:566–574, 2004.

[41] T. T. Dang-Vu, M. Desseilles, D. Petit, S. Mazza, J. Montplaisir, and P. Maquet. Neuroimaging in sleep medicine. *Sleep Med.*, 8:349–372, 2007.

[42] T. T. Dang-Vu, M. Schabus, M. Desseilles, G. Albouy, M. Boly, A. Darsaud, S. Gais, G. Rauchs, V. Sterpenich, G. Vandewalle, J. Carrier, G. Moonen, E. Balteau, C. Degueldre, A. Luxen, C. Phillips, and P. Maquet. Spontaneous neural activity during human slow wave sleep. *Proc. Natl. Acad. Sci. U. S. A.*, 105:15160–15165, 2008.

[43] T. T. Dang-Vu, M. Schabus, M. Desseilles, V. Sterpenich, M. Bonjean, and P. Maquet. Functional neuroimaging insights into the physiology of human sleep. *Sleep*, 33:1589–1603, 2010.

[44] H. Dehghani, B. R. White, B. W. Zeff, A. Tizzard, and J. P. Culver. Depth sensitivity and image reconstruction analysis of dense imaging arrays for mapping brain function with diffuse optical tomography. *Appl. Opt.*, 48:D137–D143, 2009.

[45] D. Delpy and M. Cope. Quantification in tissue near-infrared spectroscopy. *Phil. Trans. R. Soc. B*, 352:649–659, 1997.

[46] S. G. Diamond, T. J. Huppert, V. Kolehmainen, M. A. Franceschini, J. P. Kaipio, S. R. Arridge, and D. A. Boas. Dynamic physiological modeling for functional diffuse optical tomography. *NeuroImage*, 30:88–101, 2006.

[47] V. Drago, P. S. Foster, K. M. Heilman, D. Aricò, J. Williamson, P. Montagna, and R. Ferri. Cyclic alternating pattern in sleep and its relationship to creativity. *Sleep Med.*, 12:361–366, 2011.

[48] M. Dresler, S. P. Koch, R. Wehrle, V. I. Spoormaker, F. Holsboer, A. Steiger, P. G. Sämann, H. Obrig, and M. Czisch. Dreamed movement elicits activation in the sensorimotor cortex. *Curr. Biol.*, 21:1833–1837, 2011.

[49] P. D. Drummond. Adrenergic receptors in the forehead microcirculation. *Clin. Auton. Res.*, 6:23–27, 1996.

[50] P. D. Drummond. The effect of adrenergic blockade on blushing and facial flushing. *Psychophysiology*, 34:163–168, 1997.

[51] A. Duncan, J. H. Meek, M. Clemence, C. E. Elwell, L. Tyszczuk, M. Cope, and D. T. Delpy. Optical pathlength measurements on adult head, calf and forearm and the head of the newborn infant using phase resolved optical spectroscopy. *Phys. Med. Biol.*, 40:295–304, 1995.

[52] J. H. Duyn. EEG–fMRI methods for the study of brain networks during sleep. *Front. Neurol.*, 3:100, 2012.

[53] A. T. Eggebrecht, B. R. White, S. L. Ferradal, C. Chen, Y. Zhan, A. Z. Snyder, H. Dehghani, and J. P. Culver. A quantitative spatial comparison of high-density diffuse optical tomography and fMRI cortical mapping. *NeuroImage*, 61:1120–1128, 2012.

[54] A.-C. Ehlis, T. Ringel, M. Plichta, M. Richter, M. Herrmann, and A. Fallgatter. Cortical correlates of auditory sensory gating: a simultaneous near-infrared spectroscopy event-related potential study. *Neuroscience*, 159:1032–1043, 2009.

[55] C. E. Elwell. *A practical users guide to near infrared spectroscopy*. UCL, London, 1995.

[56] C. E. Elwell and C. E. Cooper. Making light work: illuminating the future of biomedical optics. *Phil. Trans. R. Soc. A*, 369:4358–4379, 2011.

[57] C. E. Elwell, R. Springett, E. Hillman, and D. T. Delpy. Oscillations in cerebral haemodynamics. Implications for functional activation studies. *Adv. Exp. Med. Biol.*, 471:57–65, 1999.

[58] G. W. Eschweiler, C. Wegerer, W. Schlotter, C. Spandl, A. Stevens, M. Bartels, and G. Buchkremer. Left prefrontal activation predicts therapeutic effects of repetitive transcranial magnetic stimulation (rTMS) in major depression. *Psychiatry Res.*, 99:161–172, 2000.

[59] S. Fantini, M. A. Franceschini, J. S. Maier, S. A. Walker, B. Barbieri, and E. Gratton. Frequency-domain multichannel optical detector for noninvasive tissue spectroscopy and oximetry. *Opt. Eng.*, 34:32–42, 1995.

[60] M. Ferrari and V. Quaresima. A brief review on the history of human functional near-infrared spectroscopy (fNIRS) development and fields of application. *NeuroImage*, 63:921–935, 2012.

[61] R. Ferri, R. Huber, D. Aricò, V. Drago, F. Rundo, M. F. Ghilardi, M. Massimini, and G. Tononi. The slow-wave components of the cyclic alternating pattern (CAP) have a role in sleep-related learning processes. *Neurosci. Lett.*, 432:228–231, 2008.

[62] M. Firbank, E. Okada, and D. T. Delpy. A theoretical study of the signal contribution of regions of the adult head to near-infrared spectroscopy studies of visual evoked responses. *NeuroImage*, 8:69–78, 1998.

[63] M. D. Fox and M. E. Raichle. Spontaneous fluctuations in brain activity observed with functional magnetic resonance imaging. *Nat. Rev. Neurosci.*, 8:700–711, 2007.

[64] P. Fox, R. Ingham, M. S. George, H. Mayberg, J. Ingham, J. Roby, C. Martin, and P. Jerabek. Imaging human intra-cerebral connectivity by PET during TMS. *NeuroReport*, 8:2787–2791, 1997.

[65] P. Fox, M. Raichle, M. Mintun, and C. Dence. Nonoxidative glucose consumption during focal physiologic neural activity. *Science*, 241:462–464, 1988.

[66] P. T. Fox, S. Narayana, N. Tandon, S. P. Fox, H. Sandoval, P. Kochunov, C. Capaday, and J. L. Lancaster. Intensity modulation of TMS-induced cortical excitation: primary motor cortex. *Hum. Brain Mapp.*, 27:478–487, 2006.

[67] M. A. Franceschini, S. Fantini, J. H. Thompson, J. P. Culver, and D. A. Boas. Hemodynamic evoked response of the sensorimotor cortex measured noninvasively with near-infrared optical imaging. *Psychophysiology*, 40:548–560, 2003.

[68] M. A. Franceschini, D. K. Joseph, T. J. Huppert, S. G. Diamond, and D. A. Boas. Diffuse optical imaging of the whole head. *J. Biomed. Opt.*, 11:054007, 2006.

[69] L. D. Gennaro and M. Ferrara. Sleep spindles: an overview. *Sleep Med. Rev.*, 7:423–440, 2003.

[70] T. Germon, P. Evans, A. Manara, N. Barnett, P. Wall, and R. Nelson. Sensitivity of near infrared spectroscopy to cerebral and extra-cerebral oxygenation changes is determined by emitter–detector separation. *J. Clin. Monit. Comput.*, 14:353–360, 1998.

[71] A. Gibson and H. Dehghani. Diffuse optical imaging. *Phil. Trans. R. Soc. A*, 367:3055–3072, 2009.

[72] A. P. Gibson, J. C. Hebden, and S. R. Arridge. Recent advances in diffuse optical imaging. *Phys. Med. Biol.*, 50:R1–R43, 2005.

[73] M. A. Grandner, N. J. Jackson, V. M. Pak, and P. R. Gehrman. Sleep disturbance is associated with cardiovascular and metabolic disorders. *J. Sleep Res.*, 21:427–433, 2012.

[74] N. M. Gregg, B. R. White, B. W. Zeff, A. J. Berger, and J. P. Culver. Brain specificity of diffuse optical imaging: improvements from superficial signal regression and tomography. *Front. Neuroenergetics*, 2:14, 2010.

[75] S. J. Groiss, H. Mochizuki, T. Furubayashi, S. Kobayashi, S. Nakatani-Enomoto, K. Nakamura, and Y. Ugawa. Quadri-pulse stimulation induces stimulation frequency dependent cortical hemoglobin concentration changes within the ipsilateral motor cortical network. *Brain Stimul.*, 2012. in press.

[76] A. Gustavsson, M. Svensson, F. Jacobi, C. Allgulander, J. Alonso, E. Beghi, R. Dodel, M. Ekman, C. Faravelli, L. Fratiglioni, B. Gannon, D. H. Jones, P. Jennum, A. Jordanova, L. Jonsson, K. Karampampa, M. Knapp, G. Kobelt, T. Kurth, R. Lieb, M. Linde, C. Ljungcrantz, A. Maercker, B. Melin, M. Moscarelli, A. Musayev, F. Norwood, M. Preisig, M. Pugliatti, J. Rehm, L. Salvador-Carulla, B. Schlehofer, R. Simon, H.-C. Steinhausen, L. J.

Stovner, J.-M. Vallat, P. Van den Bergh, J. van Os, P. Vos, W. Xu, H.-U. Wittchen, B. Jonsson, J. Olesen, and CDBE2010 Study Grp. Cost of disorders of the brain in Europe 2010. *Eur. Neuropsychopharmacol.*, 21:718–779, 2011.

[77] C. Habermehl, S. Holtze, J. Steinbrink, S. P. Koch, H. Obrig, J. Mehnert, and C. H. Schmitz. Somatosensory activation of two fingers can be discriminated with ultrahigh-density diffuse optical tomography. *NeuroImage*, 59:3201–3211, 2012.

[78] Y. Hada, M. Abo, T. Kamigana, and M. Mikami. Detection of cerebral blood flow changes during repetitive transcranial magnetic stimulation by recording hemoglobin in the brain cortex, just beneath the stimulation coil, with near-infrared spectroscopy. *NeuroImage*, 32:1226–1230, 2006.

[79] N. Hanaoka, Y. Aoyama, M. Kameyama, M. Fukuda, and M. Mikuni. Deactivation and activation of left frontal lobe during and after low-frequency repetitive transcranial magnetic stimulation over right prefrontal cortex: a near-infrared spectroscopy study. *Neurosci. Lett.*, 414:99–104, 2007.

[80] T. Hayakawa, M. Terashima, Y. Kayukawa, T. Ohta, and T. Okada. Changes in cerebral oxygenation and hemodynamics during obstructive sleep apneas. *Chest*, 109:916–921, 1996.

[81] S. Heim, S. B. Eickhoff, and K. Amunts. Specialisation in Broca's region for semantic, phonological, and syntactic fluency? *NeuroImage*, 40:1362–1368, 2008.

[82] J. Heiskala, V. Kolehmainen, T. Tarvainen, J. P. Kaipio, and S. R. Arridge. Approximation error method can reduce artifacts due to scalp blood flow in optical brain activation imaging. *J. Biomed. Opt.*, 17:096012, 2012.

[83] J. Heiskala, M. Pollari, M. Metsäranta, P. E. Grant, and I. Nissilä. Probabilistic atlas can improve reconstruction from optical imaging of the neonatal brain. *Opt. Express*, 17:14977–14992, 2009.

[84] M. J. Herrmann, T. Huter, M. Plichta, A. C. Ehlis, G. W. Alpers, A. Muhlberger, and A. J. Fallgatter. Enhancement of activity of the primary visual cortex during processing of emotional stimuli as measured with event-related functional near-infrared spectroscopy and event-related potentials. *Hum. Brain Mapp.*, 29:28–35, 2008.

[85] M. Hirose, H. Mochizuki, S. Groiss, Y. Tanji, K. Nakamura, S. Nakatani-Enomoto, H. Enomoto, M. Nishizawa, and Y. Ugawa. On-line effects of quadripulse transcranial magnetic stimulation (QPS) on the contralateral hemisphere studied with somatosensory evoked potentials and near infrared spectroscopy. *Exp. Brain Res.*, 214:577–586, 2011.

[86] V. S. Hollis. *Non-invasive monitoring of brain tissue temperature by near-infrared spectroscopy*. PhD dissertation, University College London, Department of Medical Physics and Bioengineering, 2002.

[87] F. Homae, H. Watanabe, T. Otobe, T. Nakano, T. Go, Y. Konishi, and G. Taga. Development of global cortical networks in early infancy. *J. Neurosci.*, 30:4877–4882, 2010.

[88] S. G. Horovitz, M. Fukunaga, J. A. de Zwart, P. van Gelderen, S. C. Fulton, T. J. Balkin, and J. H. Duyn. Low frequency BOLD fluctuations during resting wakefulness and light sleep: a simultaneous EEG-fMRI study. *Hum. Brain Mapp.*, 29:671–682, 2008.

[89] S. G. Horovitz and J. C. Gore. Simultaneous event-related potential and near-infrared spectroscopic studies of semantic processing. *Hum. Brain Mapp.*, 22:110–115, 2004.

[90] Y. Hoshi. Functional near-infrared spectroscopy: current status and future prospects. *J. Biomed. Opt.*, 12:062106, 2007.

[91] Y. Hoshi, S. Kosaka, Y. Xie, S. Kohri, and M. Tamura. Relationship between fluctuations in the cerebral hemoglobin oxygenation state and neuronal activity under resting conditions in man. *Neurosci. Lett.*, 245:147–150, 1998.

[92] Y. Hoshi, S. Mizukami, and M. Tamura. Dynamic features of hemodynamic and metabolic changes in the human brain during all-night sleep as revealed by near-infrared spectroscopy. *Brain Res.*, 652:257–262, 1994.

[93] Y. Hoshi and M. Tamura. Fluctuations in the cerebral oxygenation state during the resting period in functional mapping studies of the human brain. *Med. Biol. Eng. Comput.*, 35:328–330, 1997.

[94] T. J. Huppert, R. D. Hoge, S. G. Diamond, M. A. Franceschini, and D. A. Boas. A temporal comparison of BOLD, ASL, and NIRS hemodynamic responses to motor stimuli in adult humans. *NeuroImage*, 29:368–382, 2006.

[95] C. Iadecola. Neurovascular regulation in the normal brain and in Alzheimer's disease. *Nat. Rev. Neurosci.*, 5:347–360, 2004.

[96] C. Iber, S. Ancoli-Israel, A. L. Chesson, and S. F. Quan. *The AASM manual for the scoring of and associated events: rules, terminology and technical specifications*. American Academy of Sleep Medicine, 2007.

[97] M. Igawa, Y. Atsumi, K. Takahashi, S. Shiotsuka, H. Hirasawa, R. Yamamoto, A. Maki, Y. Yamashita, and H. Koizumi. Activation of visual cortex in REM sleep measured by 24-channel NIRS imaging. *Psychiatry Clin. Neurosci.*, 55:187–188, 2001.

[98] R. J. Ilmoniemi, J. Ruohonen, and J. Karhu. Transcranial magnetic stimulation–a new tool for functional imaging of the brain. *Crit. Rev. Biomed. Eng.*, 27:241–284, 1999.

[99] R. J. Ilmoniemi, J. Virtanen, J. Ruohonen, J. Karhu, H. J. Aronen, R. Näätänen, and T. Katila. Neuronal responses to magnetic stimulation reveal cortical reactivity and connectivity. *NeuroReport*, 8:3537–3540, 1997.

[100] N. K. Iwata, Y. Ugawa, E. Watanabe, Y. Yamashita, H. Koizumi, and I. Kanazawa. Interhemispheric connection between bilateral hand motor areas studied with near-infrared spectroscopic (NIRS) mapping and transcranial magnetic stimulation (TMS). *NeuroImage*, 11:S520, 2000.

[101] F. Jöbsis. Noninvasive, infrared monitoring of cerebral and myocardial oxygen sufficiency and circulatory parameters. *Science*, 198:1264–1267, 1977.

[102] J. Kaipio and E. Somersalo. Statistical and computational inverse problems. In S. S. Antman, J. E. Marsden, and L. Sirovich, editors, *Applied mathematical sciences*, volume 160. Springer Verlag, 2005.

[103] T. Katura, N. Tanaka, A. Obata, H. Sato, and A. Maki. Quantitative evaluation of interrelations between spontaneous low-frequency oscillations in cerebral hemodynamics and systemic cardiovascular dynamics. *NeuroImage*, 31:1592–1600, 2006.

[104] D. D. Kelly. Sleep and dreaming. In E. R. Kandel, J. H. Schwartz, and T. M. Jessell, editors, *Principles of neural science*, pages 792–804. Appleton & Lange, 3rd edition, 1991.

[105] L. J. Kemna and D. Gembris. Repetitive transcranial magnetic stimulation induces different responses in different cortical areas: a functional magnetic resonance study in humans. *Neurosci. Lett.*, 336:85–88, 2003.

[106] R. P. Kennan, S. G. Horovitz, A. Maki, Y. Yamashita, H. Koizumi, and J. C. Gore. Simultaneous recording of event-related auditory oddball response using transcranial near infrared optical topography and surface EEG. *NeuroImage*, 16:587–592, 2002.

[107] E. Kirilina, A. Jelzow, A. Heine, M. Niessing, H. Wabnitz, R. Brühl, B. Ittermann, A. M. Jacobs, and I. Tachtsidis. The physiological origin of task-evoked systemic artefacts in functional near infrared spectroscopy. *NeuroImage*, 61:70–81, 2012.

[108] S. P. Koch, C. Habermehl, J. Mehnert, C. H. Schmitz, S. Holtze, A. Villringer, J. Steinbrink, and H. Obrig. High-resolution optical functional mapping of the human somatosensory cortex. *Front. Neuroenergetics*, 2:12, 2010.

[109] S. P. Koch, S. Koendgen, R. Bourayou, J. Steinbrink, and H. Obrig. Individual alpha-frequency correlates with amplitude of visual evoked potential and hemodynamic response. *NeuroImage*, 41:233–242, 2008.

[110] S. P. Koch, J. Steinbrink, A. Villringer, and H. Obrig. Synchronization between background activity and visually evoked potential is not mirrored by focal hyperoxygenation: implications for the interpretation of vascular brain imaging. *J. Neurosci.*, 26:4940–4948, 2006.

[111] P. H. Koh, D. E. Glaser, G. Flandin, S. Kiebel, B. Butterworth, A. Maki, D. T. Delpy, and C. E. Elwell. Functional optical signal analysis: a software tool for near-infrared spectroscopy data processing incorporating statistical parametric mapping. *J. Biomed. Opt.*, 12:064010, 2007.

[112] S. Komssi, S. Kähkönen, and R. J. Ilmoniemi. The effect of stimulus intensity on brain responses evoked by transcranial magnetic stimulation. *Hum. Brain Mapp.*, 21:154–164, 2004.

[113] S. Komssi, P. Savolainen, J. Heiskala, and S. Kähkönen. Excitation threshold of the motor cortex estimated with transcranial magnetic stimulation electroencephalography. *NeuroReport*, 18:13–16, 2007.

[114] R. Korhonen, J. Hernandez-Pavon, J. Metsomaa, H. Mäki, R. J. Ilmoniemi, and J. Sarvas. Removal of large muscle artifacts from transcranial magnetic stimulation-evoked EEG by independent component analysis. *Med. Biol. Eng. Comput.*, 49:397–407, 2011.

[115] K. Kotilahti, I. Nissilä, M. Huotilainen, R. Mäkelä, N. Gavrielides, T. Noponen, P. Björkman, V. Fellman, and T. Katila. Bilateral hemodynamic responses to auditory stimulation in newborn infants. *NeuroReport*, 16:1373–1377, 2005.

[116] K. Kotilahti, I. Nissilä, T. Näsi, L. Lipiäinen, T. Noponen, P. Meriläinen, M. Huotilainen, and V. Fellman. Hemodynamic responses to speech and music in newborn infants. *Hum. Brain Mapp.*, 31:595–603, 2010.

[117] F. A. Kozel, F. Tian, S. Dhamne, P. E. Croarkin, S. M. McClintock, A. Elliott, K. S. Mapes, M. M. Husain, and H. Liu. Using simultaneous repetitive transcranial magnetic stimulation/functional near infrared spectroscopy (rTMS/fNIRS) to measure brain activation and connectivity. *NeuroImage*, 47:1177–1184, 2009.

[118] Y. Kubota, N. N. Takasu, S. Horita, M. Kondo, M. Shimizu, T. Okada, T. Wakamura, and M. Toichi. Dorsolateral prefrontal cortical oxygenation during REM sleep in humans. *Brain Res.*, 1389:83–92, 2011.

[119] L. J. Larson-Prior, J. M. Zempel, T. S. Nolan, F. W. Prior, A. Z. Snyder, and M. E. Raichle. Cortical network functional connectivity in the descent to sleep. *Proc. Natl. Acad. Sci. U. S. A.*, 106:4489–4494, 2009.

[120] S. Lloyd-Fox, A. Blasi, and C. E. Elwell. Illuminating the developing brain: the past, present and future of functional near infrared spectroscopy. *Neurosci. Biobehav. Rev.*, 34:269–284, 2010.

[121] H. Mäki and R. J. Ilmoniemi. Projecting out muscle artifacts from TMS-evoked EEG. *NeuroImage*, 54:2706–2710, 2011.

[122] J. B. Mandeville, J. J. Marota, C. Ayata, G. Zaharchuk, M. A. Moskowitz, B. R. Rosen, and R. M. Weisskoff. Evidence of a cerebrovascular postarteriole windkessel with delayed compliance. *J. Cereb. Blood Flow Metab.*, 19:679–689, 1999.

[123] R. Manni. Rapid eye movement sleep, non-rapid eye movement sleep, dreams, and hallucinations. *Curr. Psychiatry Rep.*, 7:196–200, 2005.

[124] P. Maquet. Functional neuroimaging of normal human sleep by positron emission tomography. *J. Sleep Res.*, 9:207–231, 2000.

[125] J. Markham, B. R. White, B. W. Zeff, and J. P. Culver. Blind identification of evoked human brain activity with independent component analysis of optical data. *Hum. Brain Mapp.*, 30:2382–2392, 2009.

[126] M. Massimini, F. Ferrarelli, R. Huber, S. K. Esser, H. Singh, and G. Tononi. Breakdown of cortical effective connectivity during sleep. *Science*, 309:2228–2232, 2005.

[127] A. Matsuo, Y. Inoue, K. Namba, and H. Chiba. Changes in cerebral hemoglobin indices in obstructive sleep apnea syndrome with nasal continuous positive airway pressure treatment. *Sleep Breath.*, 15:487–492, 2011.

[128] P. W. McCormick, M. Stewart, G. Lewis, M. Dujovny, and J. I. Ausman. Intracerebral penetration of infrared light. *J. Neurosurg.*, 76:315–318, 1992.

[129] L. Minati, I. U. Kress, E. Visani, N. Medford, and H. D. Critchley. Intra- and extra-cranial effects of transient blood pressure changes on brain near-infrared spectroscopy (NIRS) measurements. *J. Neurosci. Methods.*, 197:283–288, 2011.

[130] H. Mochizuki, T. Furubayashi, R. Hanajima, Y. Terao, Y. Mizuno, S. Okabe, and Y. Ugawa. Hemoglobin concentration changes in the contralateral hemisphere during and after theta burst stimulation of the human sensorimotor cortices. *Exp. Brain Res.*, 180:667–675, 2007.

[131] H. Mochizuki, Y. Ugawa, Y. Terao, and K. L. Sakai. Cortical hemoglobin-concentration changes under the coil induced by single-pulse TMS in humans: a simultaneous recording with near-infrared spectroscopy. *Exp. Brain Res.*, 169:302–310, 2006.

[132] J. E. Naschitz, S. Bezobchuk, R. Mussafia-Priselac, S. Sundick, D. Dreyfuss, I. Khorshidi, A. Karidis, H. Manor, M. Nagar, E. R. Peck, S. Peck, S. Storch, I. Rosner, and L. Gaitini. Pulse transit time by R-wave-gated infrared photoplethysmography: review of the literature and personal experience. *J. Clin. Monit. Comput.*, 18:333–342, 2004.

[133] I. Nissilä, K. Kotilahti, K. Fallström, and T. Katila. Instrumentation for the accurate measurement of phase and amplitude in optical tomography. *Rev. Sci. Instrum*, 73:3306–3312, 2002.

[134] I. Nissilä, T. Noponen, J. Heino, T. Kajava, and T. Katila. Diffuse optical imaging. In J. Lin, editor, *Advances in electromagnetic fields in living systems*, volume 4, pages 77–130. Springer Science, 2005.

[135] I. Nissilä, T. Noponen, K. Kotilahti, T. Tarvainen, M. Schweiger, L. Lipiäinen, S. Arridge, and T. Katila. Instrumentation and calibration methods for the multichannel measurement of phase and amplitude in optical tomograpy. *Rev. Sci. Instrum*, 76:044302, 2005.

[136] Y. Noguchi, E. Watanabe, and K. L. Sakai. An event-related optical topography study of cortical activation induced by single-pulse transcranial magnetic stimulation. *NeuroImage*, 19:156–162, 2003.

[137] H. Obrig, H. Israel, M. Kohl-Bareis, K. Uludag, R. Wenzel, B. Müller, G. Arnold, and A. Villringer. Habituation of the visually evoked potential and its vascular response: implications for neurovascular coupling in the healthy adult. *NeuroImage*, 17:1–18, 2002.

[138] H. Obrig, M. Neufang, R. Wenzel, M. Kohl, J. Steinbrink, K. Einhäupl, and A. Villringer. Spontaneous low frequency oscillations of cerebral hemodynamics and metabolism in human adults. *NeuroImage*, 12:623–639, 2000.

[139] E. Okada and D. T. Delpy. Near-infrared light propagation in an adult head model. II. Effect of superficial tissue thickness on the sensitivity of the near-infrared spectroscopy signal. *Appl. Opt.*, 42:2915–2922, 2003.

[140] A. Oliviero, V. Di Lazzaro, O. Piazza, P. Profice, M. A. Pennisi, F. Della Corte, and P. Tonali. Cerebral blood flow and metabolic changes produced by repetitive magnetic brain stimulation. *J. Neurol.*, 246:1164–1168, 1999.

[141] C. O. Olopade, E. Mensah, R. Gupta, D. Huo, D. L. Picchietti, E. Gratton, and A. Michalos. Noninvasive determination of brain tissue oxygenation during sleep in obstructive sleep apnea: a near-infrared spectroscopic approach. *Sleep*, 30:1747–1755, 2007.

[142] F. Orihuela-Espina, D. R. Leff, D. R. C. James, A. W. Darzi, and G. Z. Yang. Quality control and assurance in functional near infrared spectroscopy (fNIRS) experimentation. *Phys. Med. Biol.*, 55:3701–3724, 2010.

[143] F. Padberg and M. S. George. Repetitive transcranial magnetic stimulation of the prefrontal cortex in depression. *Exp. Neurol.*, 219:2–13, 2009.

[144] L. Parrino, R. Ferri, O. Bruni, and M. G. Terzano. Cyclic alternating pattern (CAP): the marker of sleep instability. *Sleep Med. Rev.*, 16:27–45, 2012.

[145] J. Partanen, B. Falck, J. Hasan, V. Jäntti, T. Salmi, and U. Tolonen, editors. *Kliininen neurofysiologia*. Duodecim, 1st edition, 2006.

[146] A. Pascual-Leone, J. R. Gates, and A. Dhuna. Induction of speech arrest and counting errors with rapid-rate transcranial magnetic stimulation. *Neurology*, 41:697–702, 1991.

[147] T. Paus. Inferring causality in brain images: a perturbation approach. *Phil. Trans. R. Soc. B*, 360:1109–1114, 2005.

[148] T. Paus, R. Jech, C. J. Thompson, R. Comeau, T. Peters, and A. C. Evans. Transcranial magnetic stimulation during positron emission tomography: a new method for studying connectivity of the human cerebral cortex. *J. Neurosci.*, 17:3178–3184, 1997.

[149] T. Paus, R. Jech, C. J. Thompson, R. Comeau, T. Peters, and A. C. Evans. Dose-dependent reduction of cerebral blood flow during rapid-rate transcranial magnetic stimulation of the human sensorimotor cortex. *J. Neurophysiol.*, 79:1102–1107, 1998.

[150] M. L. Peters, G. L. Godaert, R. E. Ballieux, M. van Vliet, J. J. Willemsen, F. C. Sweep, and C. J. Heijnen. Cardiovascular and endocrine responses to experimental stress: effects of mental effort and controllability. *Psychoneuroendocrinology*, 23:1–17, 1998.

[151] M. Pierro, A. Sassaroli, P. R. Bergethon, B. L. Ehrenberg, and S. Fantini. Phase-amplitude investigation of spontaneous low-frequency oscillations of cerebral hemodynamics with near-infrared spectroscopy: a sleep study in human subjects. *NeuroImage*, 63:1571–1584, 2012.

[152] F. Pizza, M. Biallas, U. Kallweit, M. Wolf, and C. L. Bassetti. Cerebral hemodynamic changes in stroke during sleep-disordered breathing. *Stroke*, 43:1951–1953, 2012.

[153] F. Pizza, M. Biallas, M. Wolf, P. O. Valko, and C. L. Bassetti. Periodic leg movements during sleep and cerebral hemodynamic changes detected by NIRS. *Clin. Neurophysiol.*, 120:1329–1334, 2009.

[154] F. Pizza, M. Biallas, M. Wolf, E. Werth, and C. L. Bassetti. Nocturnal cerebral hemodynamics in snorers and in patients with obstructive sleep apnea: a near-infrared spectroscopy study. *Sleep*, 33:205–210, 2010.

[155] M. E. Raichle and M. A. Mintun. Brain work and brain imaging. *Annu. Rev. Neurosci.*, 29:449–476, 2006.

[156] N. Roche-Labarbe, F. Wallois, E. Ponchel, G. Kongolo, and R. Grebe. Coupled oxygenation oscillation measured by NIRS and intermittent cerebral activation on EEG in premature infants. *NeuroImage*, 36:718–727, 2007.

[157] L. Rovati, G. Salvatori, L. Bulf, and S. Fonda. Optical and electrical recording of neural activity evoked by graded contrast visual stimulus. *BioMed. Eng. Online*, 6:28, 2007.

[158] C. S. Roy and C. S. Sherrington. On the regulation of the blood-supply of the brain. *J. Physiol.*, 11:85–108, 1890.

[159] R. B. Saager and A. J. Berger. Direct characterization and removal of interfering absorption trends in two-layer turbid media. *J. Opt. Soc. Am. A*, 22:1874–1882, 2005.

[160] R. B. Saager and A. J. Berger. Measurement of layer-like hemodynamic trends in scalp and cortex: implications for physiological baseline suppression in functional near-infrared spectroscopy. *J. Biomed. Opt.*, 13:034017, 2008.

[161] P. G. Sämann, R. Wehrle, D. Hoehn, V. I. Spoormaker, H. Peters, C. Tully, F. Holsboer, and M. Czisch. Development of the brain's default mode network from wakefulness to slow wave sleep. *Cereb. Cortex*, 21:2082–2093, 2011.

[162] A. Sassaroli, M. Pierro, P. Bergethon, and S. Fantini. Low-frequency spontaneous oscillations of cerebral hemodynamics investigated with near-infrared spectroscopy: a review. *Inst. Electr. Electron. Eng.*, 18:1478–1492, 2012.

[163] D. J. Schutter. Antidepressant efficacy of high-frequency transcranial magnetic stimulation over the left dorsolateral prefrontal cortex in double-blind sham-controlled designs: a meta-analysis. *Psychol. Med.*, 39:65–75, 2009.

[164] D. J. Schutter. Quantitative review of the efficacy of slow-frequency magnetic brain stimulation in major depressive disorder. *Psychol. Med.*, 40:1789–1795, 2010.

[165] M. Schweiger, I. Nissilä, D. A. Boas, and S. R. Arridge. Image reconstruction in optical tomography in the presence of coupling errors. *Appl. Opt.*, 46:2743–2756, 2007.

[166] K. H. Shelley. Photoplethysmography: beyond the calculation of arterial oxygen saturation and heart rate. *Anesth. Analg.*, 105:S31–S36, 2007.

[167] H. Shibasaki. Human brain mapping: hemodynamic response and electrophysiology. *Clin. Neurophysiol.*, 119:731–743, 2008.

[168] S. Shiotsuka, Y. Atsumi, S. Ogata, R. Yamamoto, M. Igawa, K. Takahashi, H. Hirasawa, K. Koyama, A. Maki, Y. Yamashita, H. Koizumi, and M. Toru. Cerebral blood volume in the sleep measured by near-infrared spectroscopy. *Psychiatry Clin. Neurosci.*, 52:172–173, 1998.

[169] H. R. Siebner, B. Takano, A. Peinemann, M. Schwaiger, B. Conrad, and A. Drzezga. Continuous transcranial magnetic stimulation during positron emission tomography: a suitable tool for imaging regional excitability of the human cortex. *NeuroImage*, 14:883–890, 2001.

[170] M. H. Silber, S. Ancoli-Israel, M. H. Bonnet, S. Chokroverty, M. M. Grigg-Damberger, M. Hirshkowitz, S. Kapen, S. A. Keenan, M. H. Kryger, T. Penzel, M. R. Pressman, and C. Iber. The visual scoring of sleep in adults. *J. Clin. Sleep Med.*, 3:121–131, 2007.

[171] M. Sillanpää, P. Andlin-Sobocki, and J. Lönnqvist. Costs of brain disorders in Finland. *Acta Neurol. Scand.*, 117:167–172, 2008.

[172] A. M. Speer, M. W. Willis, P. Herscovitch, M. Daube-Witherspoon, J. R. Shelton, B. E. Benson, R. M. Post, and E. M. Wassermann. Intensity-dependent regional cerebral blood flow during 1-Hz repetitive transcranial magnetic stimulation (rTMS) in healthy volunteers studied with $H_2^{15}O$ positron emission tomography: I. Effects of primary motor cortex rTMS. *Biol. Psychiatry*, 54:818–825, 2003.

[173] A. M. Speer, M. W. Willis, P. Herscovitch, M. Daube-Witherspoon, J. R. Shelton, B. E. Benson, R. M. Post, and E. M. Wassermann. Intensity-dependent regional cerebral blood flow during 1-Hz repetitive transcranial magnetic stimulation (rTMS) in healthy volunteers studied with $H_2^{15}O$ positron emission tomography: II. Effects of prefrontal cortex rTMS. *Biol. Psychiatry*, 54:826–832, 2003.

[174] A. J. Spielman, G. Zhang, C. M. Yang, P. D'Ambrosio, S. Serizawa, M. Nagata, H. von Gizycki, and R. R. Alfano. Intracerebral hemodynamics probed by near infrared spectroscopy in the transition between wakefulness and sleep. *Brain Res.*, 866:313–325, 2000.

[175] V. I. Spoormaker, M. S. Schröter, P. M. Gleiser, K. C. Andrade, M. Dresler, R. Wehrle, P. G. Sämann, and M. Czisch. Development of a large-scale functional brain network during human non-rapid eye movement sleep. *J. Neurosci.*, 30:11379–11387, 2010.

[176] G. Strangman, M. A. Franceschini, and D. A. Boas. Factors affecting the accuracy of near-infrared spectroscopy concentration calculations for focal changes in oxygenation parameters. *NeuroImage*, 18:865–879, 2003.

[177] S. Suzuki, S. Takasaki, T. Ozaki, and Y. Kobayashi. Tissue oxygenation monitor using NIR spatially resolved spectroscopy. In *Proc. SPIE: Optical Tomography and Spectroscopy of Tissue III*, volume 3597, pages 582–592, 1999.

[178] I. Tachtsidis, C. E. Elwell, T. S. Leung, C. W. Lee, M. Smith, and D. T. Delpy. Investigation of cerebral haemodynamics by near-infrared spectroscopy in young healthy volunteers reveals posture-dependent spontaneous oscillations. *Physiol. Meas.*, 25:437–445, 2004.

[179] I. Tachtsidis, T. S. Leung, A. Chopra, P. H. Koh, C. B. Reid, and C. E. Elwell. False positives in functional near-infrared topography. *Adv. Exp. Med. Biol.*, 645:307–314, 2009.

[180] T. Takahashi, Y. Takikawa, R. Kawagoe, S. Shibuya, T. Iwano, and S. Kitazawa. Influence of skin blood flow on near-infrared spectroscopy signals measured on the forehead during a verbal fluency task. *NeuroImage*, 57:991–1002, 2011.

[181] M. Takeuchi, E. Hori, K. Takamoto, A. Tran, K. Satoru, A. Ishikawa, T. Ono, S. Endo, and H. Nishijo. Brain cortical mapping by simultaneous recording of functional near infrared spectroscopy and electroencephalograms from the whole brain during right median nerve stimulation. *Brain Topogr.*, 22:197–214, 2009.

[182] T. Tarvainen, V. Kolehmainen, M. Vauhkonen, A. Vanne, A. P. Gibson, M. Schweiger, S. R. Arridge, and J. P. Kaipio. Computational calibration method for optical tomography. *Appl. Opt.*, 44:1879–1888, 2005.

[183] T. Tarvainen, M. Vauhkonen, and S. R. Arridge. Gauss–Newton reconstruction method for optical tomography using the finite element solution of the radiative transfer equation. *J. Quant. Spectrosc. Radiat. Transf.*, 109:2767–2778, 2008.

[184] M. G. Terzano and L. Parrino. Origin and significance of the cyclic alternating pattern (CAP). *Sleep Med. Rev.*, 4:101–123, 2000.

[185] M. G. Terzano, L. Parrino, A. Sherieri, R. Chervin, S. Chokroverty, C. Guilleminault, M. Hirshkowitz, M. Mahowald, H. Moldofsky, A. Rosa, R. Thomas, and A. Walters. Atlas, rules, and recording techniques for the scoring of cyclic alternating pattern (CAP) in human sleep. *Sleep Med.*, 2:537–553, 2002.

[186] R. H. Thomson, Z. J. Daskalakis, and P. B. Fitzgerald. A near infra-red spectroscopy study of the effects of pre-frontal single and paired pulse transcranial magnetic stimulation. *Clin. Neurophysiol.*, 122:378–382, 2011.

[187] R. H. Thomson, J. J. Maller, Z. J. Daskalakis, and P. B. Fitzgerald. Blood oxygenation changes resulting from trains of low frequency transcranial magnetic stimulation. *Cortex*, 48:487–491, 2012.

[188] F. Tian, H. Niu, B. Khan, G. Alexandrakis, K. Behbehani, and H. Liu. Enhanced functional brain imaging by using adaptive filtering and a depth compensation algorithm in diffuse optical tomography. *IEEE Trans. Med. Imag.*, 30:1239–1251, 2011.

[189] Y. Tong and B. D. Frederick. Time lag dependent multimodal processing of concurrent fMRI and near-infrared spectroscopy (NIRS) data suggests a global circulatory origin for low-frequency oscillation signals in human brain. *NeuroImage*, 53:553–564, 2010.

[190] Y. Tong, L. M. Hocke, and B. d. Frederick. Isolating the sources of widespread physiological fluctuations in functional near-infrared spectroscopy signals. *J. Biomed. Opt.*, 16:106005, 2011.

[191] M. Uchida-Ota, N. Tanaka, H. Sato, and A. Maki. Intrinsic correlations of electroencephalography rhythms with cerebral hemodynamics during sleep transitions. *NeuroImage*, 42:357–368, 2008.

[192] K. Uludağ, M. Kohl, J. Steinbrink, H. Obrig, and A. Villringer. Cross talk in the Lambert–Beer calculation for near-infrared wavelengths estimated by Monte Carlo simulations. *J. Biomed. Opt.*, 7:51–59, 2002.

[193] K. Uludağ, J. Steinbrink, A. Villringer, and H. Obrig. Separability and cross talk: optimizing dual wavelength combinations for near-infrared spectroscopy of the adult head. *NeuroImage*, 22:583–589, 2004.

[194] A. Valipour, A. D. McGown, H. Makker, C. O'Sullivan, and S. G. Spiro. Some factors affecting cerebral tissue saturation during obstructive sleep apnoea. *Eur. Respir. J.*, 20:444–450, 2002.

[195] P. van der Zee, M. Cope, S. R. Arridge, M. Essenpreis, L. A. Potter, A. D. Edwards, J. S. Wyatt, D. C. McCormick, S. C. Roth, E. O. Reynolds, and D. T. Delpy. Experimentally measured optical pathlengths for the adult head, calf and forearm and the head of the newborn infant as a function of inter optode spacing. *Adv. Exp. Med. Biol.*, 316:143–153, 1992.

[196] J. Virtanen, T. Noponen, K. Kotilahti, J. Virtanen, and R. J. Ilmoniemi. Accelerometer-based method for correcting signal baseline changes caused by motion artifacts in medical near-infrared spectroscopy. *J. Biomed. Opt.*, 16:087005, 2011.

[197] J. Virtanen, T. Noponen, and P. Meriläinen. Comparison of principal and independent component analysis in removing extracerebral interference from near-infrared spectroscopy signals. *J. Biomed. Opt.*, 14:054032, 2009.

[198] J. Virtanen, T. Noponen, T. Salmi, J. Toppila, and P. Meriläinen. Impaired cerebral vasoreactivity may cause cerebral blood volume dip following obstructive sleep apnea termination. *Sleep Breath.*, 16:309–312, 2012.

[199] F. Wallois, M. Mahmoudzadeh, A. Patil, and R. Grebe. Usefulness of simultaneous EEG–NIRS recording in language studies. *Brain Lang.*, 121:110–123, 2012.

[200] E. M. Wassermann, C. M. Epstein, U. Ziemann, V. Walsh, T. Paus, and S. H. Lisanby, editors. *The Oxford handbook of transcranial magnetic stimulation*. Oxford University Press, 1st edition, 2008.

[201] E. M. Wassermann and T. Zimmermann. Transcranial magnetic brain stimulation: therapeutic promises and scientific gaps. *Pharmacol. Ther.*, 133:98–107, 2012.

[202] B. R. White, A. Z. Snyder, A. L. Cohen, S. E. Petersen, M. E. Raichle, B. L. Schlaggar, and J. P. Culver. Resting-state functional connectivity in the human brain revealed with diffuse optical tomography. *NeuroImage*, 47:148–156, 2009.

[203] M. Wolf, M. Ferrari, and V. Quaresima. Progress of near-infrared spectroscopy and topography for brain and muscle clinical applications. *J. Biomed. Opt.*, 12:062104, 2007.

[204] World Health Organization. *Medical Devices: managing the mismatch. An Outcome of the Priority Medical Devices Project*. World Health Organization, Geneva, Switzerland, 2010.

[205] T. Yamada, S. Umeyama, and K. Matsuda. Separation of fNIRS signals into functional and systemic components based on differences in hemodynamic modalities. *PLoS ONE*, 7:e50271, 2012.

[206] K. Yamanaka, B. Yamagata, H. Tomioka, S. Kawasaki, and M. Mimura. Transcranial magnetic stimulation of the parietal cortex facilitates spatial working memory: near-infrared spectroscopy study. *Cereb. Cortex*, 20:1037–1045, 2010.

[207] Y. Yamashita, A. Maki, and H. Koizumi. Wavelength dependence of the precision of noninvasive optical measurement of oxy-, deoxy-, and total-hemoglobin concentration. *Med. Phys.*, 28:1108–1114, 2001.

[208] B. W. Zeff, B. R. White, H. Dehghani, B. L. Schlaggar, and J. P. Culver. Retinotopic mapping of adult human visual cortex with high-density diffuse optical tomography. *Proc. Natl. Acad. Sci. U. S. A.*, 104:12169–12174, 2007.

[209] J. Zhai, T. Li, Z. Zhang, and H. Gong. Hemodynamic and electrophysiological signals of conflict processing in the Chinese-character Stroop task: a simultaneous near-infrared spectroscopy and event-related potential study. *J. Biomed. Opt.*, 14:054022, 2009.

[210] Q. Zhang, E. N. Brown, and G. E. Strangman. Adaptive filtering for global interference cancellation and real-time recovery of evoked brain activity: a Monte Carlo simulation study. *J. Biomed. Opt.*, 12:044014, 2007.

[211] Q. Zhang, G. E. Strangman, and G. Ganis. Adaptive filtering to reduce global interference in non-invasive NIRS measures of brain activation: how well and when does it work? *NeuroImage*, 45:788–794, 2009.

[212] Y. Zhang, D. H. Brooks, M. A. Franceschini, and D. A. Boas. Eigenvector-based spatial filtering for reduction of physiological interference in diffuse optical imaging. *J. Biomed. Opt.*, 10:011014, 2005.

Aalto-DD 45/2013

ISBN 978-952-60-5069-0
ISBN 978-952-60-5070-6 (pdf)
ISSN-L 1799-4934
ISSN 1799-4934
ISSN 1799-4942 (pdf)

Aalto University
School of Science
Dept. of Biomedical Engineering and Computational Science
www.aalto.fi

BUSINESS +
ECONOMY

ART +
DESIGN +
ARCHITECTURE

SCIENCE +
TECHNOLOGY

CROSSOVER

**DOCTORAL
DISSERTATIONS**